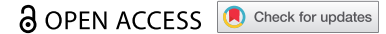


RESEARCH PAPER



## Direct homophilic interaction of LAMP2A with the two-domain architecture revealed by site-directed photo-crosslinks and steric hindrances in mammalian cells

Kazue Terasawa<sup>a\*</sup>, Yuji Kato<sup>b\*</sup>, Yuta Ikami<sup>c</sup>, Kensaku Sakamoto<sup>d</sup>, Kazumasa Ohtake<sup>d</sup>, Seisuke Kusano<sup>e</sup>, Yuri Tomabechi<sup>f</sup>, Mutsuko Kukimoto-Niino<sup>f</sup>, Mikako Shirouzu<sup>f</sup>, Jun-Lin Guan<sup>g</sup>, Toshihide Kobayashi<sup>h</sup>, Takanori Iwata<sup>b</sup>, Tetsuro Watabe<sup>a</sup>, Shigeyuki Yokoyama<sup>e</sup>, and Miki Hara-Yokoyama<sup>a</sup>

<sup>a</sup>Department of Biochemistry, Graduate School of Medical and Dental Sciences, Tokyo Medical and Dental University (TMDU), Tokyo, Japan; <sup>b</sup>Department of Periodontology, Graduate School of Medical and Dental Sciences, Tokyo Medical and Dental University (TMDU), Tokyo, Japan; <sup>c</sup>Department of Oral and Maxillofacial Surgery, Graduate School of Medical and Dental Sciences, Tokyo Medical and Dental University (TMDU), Tokyo, Japan; <sup>d</sup>Laboratory for Nonnatural Amino Acid Technology, RIKEN Center for Biosystems Dynamics Research, Yokohama, Japan; <sup>e</sup>RIKEN Cluster for Science, Technology and Innovation Hub, Yokohama, Japan; <sup>f</sup>Laboratory for Protein Function and Structural Biology, RIKEN Center for Biosystems Dynamics Research, Yokohama, Japan; <sup>g</sup>Department of Cancer Biology, University of Cincinnati College of Medicine, Cincinnati, OH, USA; <sup>h</sup>Laboratoire de Biomagerie et Pathologies, UMR 7021 CNRS, Université de Strasbourg, Illkirch, France

### ABSTRACT

LAMP1 (lysosomal-associated membrane protein 1) and LAMP2 are the most abundant protein components of lysosome membranes. Both LAMPs have common structures consisting of a large luminal domain composed of two domains (N-domain and C-domain, which are membrane-distal and -proximal, respectively), both with the  $\beta$ -prism fold, a transmembrane domain, and a short cytoplasmic tail. LAMP2 is involved in various aspects of autophagy, and reportedly forms high-molecular weight complexes at the lysosomal membrane. We previously showed that LAMP2 molecules coimmunoprecipitated with each other, but whether the homophilic interaction is direct or indirect has remained to be elucidated. In the present study, we demonstrated the direct homophilic interaction of mouse LAMP2A molecules, using expanded genetic code technologies that generate photo-crosslinking and/or steric hindrance at specified interfaces. Specifically, the results suggested that LAMP2A molecules assemble by facing each other with one side of the  $\beta$ -prism (defined as side A) of the C-domains. The N-domain truncation, which increased the coimmunoprecipitation of LAMP2A molecules in our previous study, permitted the nonspecific involvement of both sides of the  $\beta$ -prism (side A and side B). Thus, the presence of the N-domain restricts the LAMP2A interactions to side A-specific. The truncation of LAMP2A impaired the recruitment of GAPDH (a CMA-substrate) fused to the HaloTag protein to the surface of late endosomes/lysosomes (LE/Lys) and affected a process that generates LE/Lys. The present study revealed that the homophilic interaction of LAMP2A is direct, and the side A-specific, homophilic interaction of LAMP2A is required for the functional aspects of LAMP2A.

**Abbreviations:** Aloc-Lys: *N*<sup>ε</sup>-allyloxycarbonyl-L-lysine; CMA: chaperone-mediated autophagy; FFE: free-flow electrophoresis; GAPDH-HT: glyceraldehyde-3-phosphate dehydrogenase fused to HaloTag protein; LAMP1: lysosomal-associated membrane protein 1; LAMP2A: lysosomal-associated membrane protein 2A; LBPA: lysobisphosphatidic acid; LE/Lys: late endosome/lysosomes; MEFs: mouse embryonic fibroblasts; *p*Bpa: *p*-benzoyl-L-phenylalanine

### ARTICLE HISTORY

Received 25 April 2020  
Revised 24 March 2021  
Accepted 26 March 2021



### KEYWORDS

Chaperone-mediated autophagy; expanded genetic codes; GAPDH-HT; lysosomes; photo-crosslinking; protein assembly

### Introduction


Lysosomes are principally responsible for intracellular digestion. Although various acid hydrolases within lysosomes are responsible for this degradative process, lysosomal membranes also play crucial roles to fulfill the actions of lysosomes [1]. LAMP1/lgp120/CD107a (lysosomal-associated membrane protein 1) and LAMP2/lgp110/CD107b are the most abundant protein components of lysosome membranes [2,3]. LAMPs are type I transmembrane proteins composed of

a large, heavily glycosylated luminal domain, a transmembrane domain, and a short C-terminal cytoplasmic tail (Figure 1A). The luminal domains of both LAMP1 and LAMP2 are composed of two domains, the membrane-distal domain (the N-domain) and the membrane-proximal domain (the C-domain), which are connected by the linker region. In contrast, the luminal domains of other members of the LAMP family proteins lack one of the two domains. Each domain has the unique  $\beta$ -prism fold structure (Fig. S1A) [4,5].

**CONTACT** Miki Hara-Yokoyama  [m.yokoyama.bch@tmd.ac.jp](mailto:m.yokoyama.bch@tmd.ac.jp)  Department of Biochemistry, Graduate School of Medical and Dental Sciences, Tokyo Medical and Dental University (TMDU), Yushima 1-5-45, Bunkyo-ku, Tokyo 113-8549, Japan

\*These authors are contributed equally to this work.

‡Present address: (Kazue Terasawa): LiberoThera Co., Ltd., 2-3-11 Nihonbashi-honcho, Chuo-ku, 103-0032, Japan.

 Supplemental data for this article can be accessed [here](#).

© 2021 The Author(s). Published by Informa UK Limited, trading as Taylor & Francis Group.  
This is an Open Access article distributed under the terms of the Creative Commons Attribution-NonCommercial-NoDerivatives License (<http://creativecommons.org/licenses/by-nc-nd/4.0/>), which permits non-commercial re-use, distribution, and reproduction in any medium, provided the original work is properly cited, and is not altered, transformed, or built upon in any way.

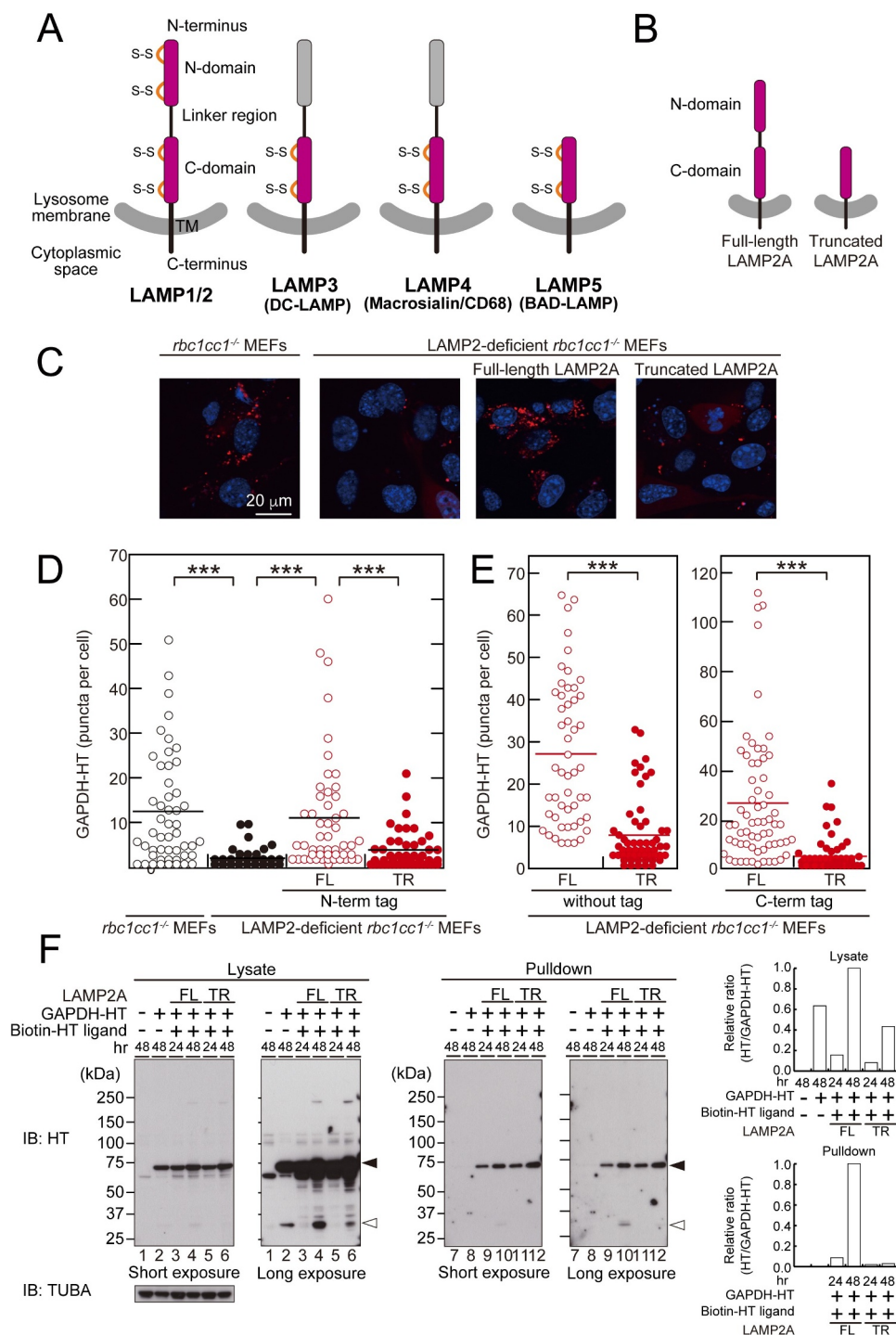


**Figure 1.** The N-domain truncation of mouse LAMP2A impairs the CMA activity. (A) Domain architectures and orientations of five LAMP family proteins. The core domain common to LAMPs 1–5 has four conserved cysteine residues that can form two disulfide bonds (pink). Both LAMP1 and LAMP2 have two core domains, whereas LAMP3 and LAMP4 have a mucin-like domain (gray) in addition to the core domain [50,51] and LAMP5 is composed of the single core domain [52]. (B) Schematic representations of the full-length and N-domain truncated LAMP2A proteins used in this study. (C, D) *rbc1cc1*<sup>-/-</sup> MEFs either with or without LAMP2 (generated by guide RNA #2) were transfected with GAPDH-HT. The full-length or truncated FLAG-LAMP2A (the N-terminally FLAG-tagged) was expressed together with GAPDH-HT in LAMP2-deficient *rbc1cc1*<sup>-/-</sup> MEFs. The fluorescence images after labeling with TMR-HT ligand (red) for 18–20 h are shown. Nuclei were stained with Hoechst (blue). (D) Quantitative analysis of GAPDH-HT puncta. *n* = 50, 42, 51, 47. \*\*\**P* < 0.001. Essentially the same results were obtained in three independent experiments, including one using guide RNA #1. (E) Quantitative analysis of GAPDH-HT puncta upon expression of the full-length or truncated LAMP2A, which is not tagged (left panel, *n* = 51, 59), or the C-terminally FLAG-tagged LAMP2A (right panel, *n* = 64, 53), in LAMP2-deficient *rbc1cc1*<sup>-/-</sup> MEFs. (F) GAPDH-HT was transiently expressed in *rbc1cc1*<sup>-/-</sup> MEFs (lane 2) or in the clones of LAMP2-deficient *rbc1cc1*<sup>-/-</sup> MEFs stably expressing the full-length (FL) or truncated (TR) N-terminally FLAG-tagged LAMP2A (lanes 3, 4 and 5, 6, respectively). As a control, *rbc1cc1*<sup>-/-</sup> MEFs were used without transfection of GAPDH-HT (lane 1). Twenty-four hours after the transfection of GAPDH-HT, biotin-HT ligand was added to the medium and the cells were cultured for an additional 24 h (lanes 3–6). The proteins in the lysates and retrieved by NeutrAvidin beads (Pulldown) were analyzed by immunoblotting using an anti-HaloTag protein antibody, and reprobred with an anti-tubulin antibody. Closed and open triangles show GAPDH-HT (70 kDa) and likely the HT protein (30 kDa), respectively. Essentially the same results were obtained in an independent experiment. See also Fig. S2.

Mice deficient in both LAMP1 and LAMP2 are embryonic lethal between days 14.5 to 16.5 [6]. Thus, LAMPs are physiologically essential proteins. On the other hand, mice deficient in LAMP1 are viable and fertile [7], whereas the LAMP2 deficiency increases postnatal mortality between 20 and 40 days of age, and the surviving mice are smaller than wild-type mice [8]. Thus, although LAMP1 and LAMP2 functionally compensate for each other, the severe phenotypes due to the LAMP2 deficiency imply that LAMP2 plays more crucial roles in some aspects of lysosome functions than LAMP1.

In the LAMP2-deficient mice, autophagic vacuoles accumulate in several tissues, suggesting that LAMP2 is important for macroautophagy/autophagy [8]. There are three isoforms of LAMP2, known as LAMP2A, LAMP2B, and LAMP2C and arising from the alternative splicing of a single *Lamp2* gene, which have the common luminal domain and differ primarily in the sequences of their transmembrane and cytoplasmic regions (Fig. S1D) [9]. LAMP2A functions as a receptor of chaperone-mediated autophagy (CMA), in which cytoplasmic proteins are transported into lysosomes for degradation [10]. LAMP2B is highly expressed in human cardiomyocytes, where its deficiency impairs the autophagosome-lysosome fusion to cause the cardiomyopathy in Danon disease [11,12]. LAMP2C is involved in the processes of incorporating and degrading DNA and RNA within lysosomes (RNautophagy/DNautophagy) [13,14]. Accordingly, LAMP2s contribute to various aspects of autophagy.

We previously reported that the N- and C-domains form the unique  $\beta$ -prism fold (Fig. S1A) [4], a triangular prism composed of  $\beta$ -sheets, which is similar to the domain structure of the dendritic cell-specific-LAMP (DC-LAMP, LAMP3) [5]. Thus, the  $\beta$ -prism fold is the conserved aspect of this LAMP family. In addition, we found that the N-domain truncation decreased the coimmunoprecipitation of LAMP1 molecules, whereas the truncation increased that of LAMP2 molecules [4]. The results suggested that the mode of LAMP2 assembly is related to the importance of LAMP2 in autophagy.

Several biochemical approaches, such as native gel electrophoresis, size exclusion chromatography, and sucrose density gradient ultracentrifugation, have demonstrated the association of the LAMPs solubilized from tissues or cultured cells with high-molecular-weight complexes [4,15]. Our previous coimmunoprecipitation-based study supported the homophilic interaction between LAMPs [4]. However, the question of whether the association of the LAMPs is direct or mediated by other molecules has remained to be answered.

Site-specific photo-crosslinking is suitable to analyze protein assemblies within cells [16–18]. This method is based on expanded genetic code technologies: a photo-reactive crosslinker (*p*-benzoyl-L-phenylalanine, *p*Bpa), a non-natural amino acid, is introduced at the position specified by the *amber* codon UAG, during translation with an *amber* suppressor tRNA and an engineered tyrosyl-tRNA synthetase that can charge the tRNA with *p*Bpa [19–21]. Exposure of the cells to 365-nm light (UV-C) causes the *p*Bpa-incorporated protein to crosslink with any molecule in the proximity of the *p*Bpa. Using this method, we previously demonstrated the tetrameric assembly of CD38 on the cell surface [22].

In the present study, we applied the site-specific photo-crosslinking method to mouse LAMP2A and showed the direct homophilic interaction between LAMP2A molecules within cells, for the first time. We also used the expanded genetic code technologies for the site-specific steric hindrance. We found that the C-domains of LAMP2A face one side of the  $\beta$ -prism (side A, shown in Fig. S1A) toward each other in the homophilic interaction. By contrast, when LAMP2A lacked the N-domain and the linker region, both sides of the  $\beta$ -prism (side A and side B) contributed to the homophilic interaction. The truncation of LAMP2A decreased the recruitment of a CMA substrate (GAPDH [glyceraldehyde-3-phosphate dehydrogenase] [23]) fused to the HaloTag protein (GAPDH-HT), from the cytosol to the surface of late endosome/lysosomes (LE/Lys). In addition, the truncation likely affected a process in LE/Lys generation. Accordingly, the present study demonstrated that the presence of the two domains in the luminal domain of LAMP2A is required for the side A-specific homophilic interaction and the functional aspects of LAMP2A.

## Results

### **The N-domain truncation of mouse LAMP2A impairs the CMA activity, based on the LAMP2A-dependent recruitment of a CMA substrate, GAPDH-HT, to the surface of LE/Lys**

We previously reported that the N-domain truncation of mouse LAMP2A appreciably increased the coimmunoprecipitation between the LAMP2A molecules [4]. In the present study, we investigated the functional aspects of the N-domain truncation, using LAMP2A lacking the N-domain and the linker region (referred to as truncated LAMP2A, hereafter) (Figure 1B).

The CMA activity depends on LAMP2A [24]. Seki *et al.* established a novel fluorescence-based method to evaluate CMA activities, using GAPDH-HT [25,26]. The cytosolic GAPDH-HT was fluorescently labeled by a brief extracellular application of a TMR HaloTag ligand. The formation of GAPDH-HT puncta is due to the recruitment of GAPDH-HT from the cytosol to the LE/Lys surface, in the process of CMA and microautophagy. Since microautophagy is independent of LAMP2A [27], the LAMP2A-dependent formation of GAPDH-HT puncta is used to assess the CMA activity [26].

The full-length or truncated LAMP2A was transiently expressed together with GAPDH-HT in mouse embryonic fibroblasts (MEFs) deficient in both LAMP2 and RB1CC1/FIP200 (RB1-inducible coiled-coil 1) (Fig. S2A). Because the factors necessary to translocate GAPDH-HT into LE/Lys are likely to be insufficient for a large excess of LAMP2A upon transient transfection, the recruited GAPDH-HT may accumulate on the surface of LE/Lys. *rbc1cc1*<sup>-/-</sup> MEFs were used to exclude the involvement of macroautophagy [28]. Since the C-terminal tail of LAMP2A is crucial for the CMA activity [24], the N-terminally FLAG-tagged LAMP2A with an intact C-terminal tail was used. The expression levels of GAPDH-HT and LAMP2A were not significantly different with either the full-length or truncated LAMP2A (Figs. S2B–D).

Consistent with the previous studies [25,26], the number of GAPDH-HT puncta per cell in *rbc1cc1*<sup>-/-</sup> MEFs was larger than that in LAMP2-deficient *rbc1cc1*<sup>-/-</sup> MEFs (Figure 1C,D). When the full-length LAMP2A was expressed in LAMP2-deficient *rbc1cc1*<sup>-/-</sup> MEFs, the fluorescence signals due to GAPDH-HT and Cell-Navigator largely overlapped, suggesting the recruitment of GAPDH-HT to the surface of acidic LE/Lys compartments (Fig. S2E). The translocation of a CMA substrate protein to LE/Lys depends on the presence of a pentapeptide motif with amino acid residues biochemically related to KFERQ [29]. GAPDH harbors VKAEN within the loop region on the surface of GAPDH (PDB 1U8F) [30], which is consistent with the CMA motif [29]. When a 2-aa mutation was introduced to GAPDH-HT (GAPDH-HT<sup>E63A,N64A</sup>), the puncta formation was appreciably reduced (Fig. S2F), showing that the translocation of GAPDH-HT to the LE/Lys surface by the expression of full-length LAMP2A is a CMA-relevant process.

The expression of the full-length LAMP2A restored the number of GAPDH-HT puncta in LAMP2-deficient *rbc1cc1*<sup>-/-</sup> MEFs, whereas the truncated LAMP2A was significantly less effective (Figure 1C,D). Similar results were obtained with combinations of the full-length and truncated LAMP2A, which were untagged or C-terminally FLAG-tagged (Figure 1E, left and right, respectively). Thus, the truncation of the N-domain of LAMP2A apparently impaired the recruitment of GAPDH-HT to LE/Lys in the CMA process.

### **The N-domain truncation of LAMP2A decreases the HaloTag protein release from GAPDH-HT**

In order to investigate the effect of the N-domain truncation further, we generated clones stably expressing either the full-length or truncated FLAG-LAMP2A in LAMP2-deficient *rbc1cc1*<sup>-/-</sup> MEFs. After the cells were transfected with the GAPDH-HT, the GAPDH-HT was labeled by a brief extracellular application of a biotin HaloTag ligand. The cells were cultured further for 24 h, and the lysates and the biotinylated materials retrieved by NeutrAvidin Agarose were analyzed by immunoblotting with an anti-HaloTag protein antibody (Figure 1F). After the cells were cultured for 48 h, the 30 kDa species was detected by an anti-HaloTag antibody (Figure 1F, lanes 2, 4, 6, 10 in long exposure). The 30 kDa species was most prominently observed in the case of the full-length LAMP2A clone in the lysates (Figure 1F, lane 4 in long exposure) and retrieved by NeutrAvidin Agarose, suggesting that the 30 kDa species is derived from GAPDH-HT and most likely the HaloTag protein (Figure 1F, lane 10 in long exposure).

It should be noted that, in the macroautophagy-competent MEFs, the 30 kDa species was hardly observed (Fig. S2G, lanes 4 and 5). The result can be explained by the fact that macroautophagy causes the complete degradation of materials entrapped within autophagosomes (schematically shown in Fig. S2H, case 3). On the other hand, the 30 kDa species was detected when E64d (CTSB [cathepsin B] and CTSL inhibitor) was present in the culture medium (Fig. S2G, lane 6). Although the cytosolic protease activities should be much lower than those in lysosomes, these activities were

previously reported [31,32]. We noticed that the HaloTag protein, derived from the haloalkane dehalogenase enzyme from *Rhodococcus rhodochrous* [33], has no CMA motif. Thus, it is conceivable that, after the chaperone-mediated recruitment of GAPDH-HT to the surface of LE/Lys, the GAPDH portion of GAPDH-HT with the CMA motif is unfolded and enters the lysosome lumen prior to the HaloTag protein. In this CMA intermediate, the linker region between GAPDH and the HaloTag protein would be susceptible to an attack by cytosolic proteases, especially since the inhibition of the lysosomal proteolytic activities by E64d thereby attenuated the completion of the CMA processes (shown by a red arrow in Fig. S2H, case 2).

By contrast, in the LAMP2A-overexpressing *rbc1cc1*<sup>-/-</sup> MEFs, the 30-kDa species was detected after a 48-h incubation without or with E64d (Fig. S2G, lanes 1–3). This result suggested that the 30 kDa protein was derived from the GAPDH-HT recruited to the LE/Lys surface by the aid of chaperones, rather than from the CMA intermediate (Fig. S2H, case 1). The recruited GAPDH-HT may accumulate on the surface of LE/Lys, since the factors necessary to convert the recruited GAPDH-HT to the next intermediate state are likely to be insufficient in the presence of a large excess of LAMP2A.

The ratio of the 30 kDa protein to the GAPDH-HT in the case of the truncated FLAG-LAMP2A clone was less than that in the case of the full-length FLAG-LAMP2A clone, in both the lysate and the retrieved fraction (Figure 1F). These results suggested that the N-domain truncation of LAMP2A decreased the recruitment of GAPDH-HT to the LE/Lys surface, which is consistent with the decrease in the number of GAPDH-HT puncta, as shown in Figure 1D.

### **Expression of N-domain truncated LAMP2A impairs the generation of mature LE/Lys**

We investigated whether the truncation of the N-domain and the linker region affects the intracellular localization of LAMP2A. The clones expressing either full-length or truncated FLAG-LAMP2A were co-stained with anti-LAMP2A and anti-lysobisphosphatidic acid (LBPA, an LE/Lys marker [34]) antibodies (Fig. S2I). The full-length FLAG-LAMP2A and LBPA were distributed similarly and associated with the same vesicles (Fig. S2J, white triangles in upper panels). Conversely, the distribution of the truncated FLAG-LAMP2A was comparatively more diffuse than that of the full-length FLAG-LAMP2A (Fig. S2I). However, some of the truncated FLAG-LAMP2A and LBPA molecules were associated with the same vesicles (Fig. S2J, white triangles in lower panels), suggesting that the truncation does not completely inhibit the localization of LAMP2A to LE/Lys. The vesicles with the majority of the truncated FLAG-LAMP2A were associated with a smaller amount of LBPA (Fig. S2J, yellow triangles in lower panels). Thus, the truncated LAMP2A is localized to vesicles that are at least related to LE/Lys. When the full-length or truncated FLAG-LAMP2A clones were stained with Cell-Navigator, the numbers of positive vesicles per cell were not significantly different (Fig. S2K, left graph).

Conversely, the size of positive vesicles in the truncated FLAG-LAMP2A clone was smaller (Fig. S2K, right graph).

More diffuse distributions of the truncated FLAG-LAMP2A were also observed when the untagged or C-terminally FLAG-tagged LAMP2A was stably expressed in LAMP2-deficient *rbclcc1*<sup>-/-</sup> MEFs (Figs. S2L, M, respectively).

Considering that the LE/Lys vesicles gain LBPA during endosome maturation [35], the expression of the truncated LAMP2A may impair the generation of mature LE/Lys vesicles. Taken together, the N-domain truncation apparently influences the maturation of LE/Lys, in addition to impairing GAPDH-HT recruitment to the LE/Lys surface during the CMA process.

### Direct homophilic interaction of mouse LAMP2A revealed by site-specific crosslinking

We next examined whether the putative homophilic interaction of mouse LAMP2A occurs directly or indirectly. First of all, the isolated N- and C-domains of LAMP2A were tested for their homophilic oligomerization. The domains were expressed as secreted proteins and purified as described previously [4]. Both domains existed as monomers, as revealed by size exclusion chromatography (Fig. S1B). The N- and C-domains of LAMP1 also existed as monomers (Fig. S1B). Therefore, these luminal domains in isolation have no abilities to associate with themselves, suggesting that the transmembrane structures are required for the multimerization of LAMPs.

Thus, we introduced the photo-reactive crosslinker amino acid (*p*Bpa) at the position specified by the UAG mutation within the membrane-proximal, C-domain of the full-length LAMP2A, according to the methods of Hino *et al.* [19,20] (Figure 2A). To confirm the completion of the translation of the LAMP2A variant by the exogenous UAG-translating machinery, it was tagged with FLAG at the C terminus. Each variant LAMP2A-FLAG protein was designed to have the photo-crosslinker at one of nine positions covering sides A and B of the  $\beta$ -prism of the C-domain (Figure 2B). The *p*Bpa-containing variants of LAMP2A-FLAG were coexpressed with the wild-type LAMP2A-MYC in HEK293c18 cells. To avoid damage to the cells, the duration of UV irradiation was just enough to detect photo-crosslinks. The cells were then lysed, and the lysates were subjected to immunoprecipitation with an anti-FLAG antibody.

As shown in Figure 2C, in addition to the monomer of LAMP2A-MYC (75–100 kDa), UV-crosslinked products containing LAMP2A-MYC were observed at around 190 kDa for all of the test positions. Although long irradiation durations over several hours reportedly increase the efficiency of photo-crosslinking [36], in this study the irradiation was shorter, to avoid impairment of the cell viability. Thus, the amounts of the crosslinked products may be less than those of the coimmunoprecipitated monomers. The band intensities of the six variants, with *p*Bpa on side A (LAMP2A-FLAG<sup>T235X</sup>, LAMP2A-FLAG<sup>K252X</sup>, LAMP2A-FLAG<sup>P261X</sup>, LAMP2A-FLAG<sup>P272X</sup> and LAMP2A-FLAG<sup>R278X</sup>) and on the loop between sides A and B (LAMP2A-FLAG<sup>L330X</sup>) (X: *p*Bpa), were clearly higher than those of the others. Therefore, the

crosslinking occurred mainly on side A. This site-specific crosslinking demonstrated that the homophilic interaction of mouse LAMP2A is direct, and the C-domain contributes to it. Although these crosslinking residues of one protein molecule are certainly close to its partner molecule, this does not necessarily mean that the residues originally located at these positions are directly involved in the interactions with the partner.

### Side A regions of the C-domains face each other in the homophilic interaction of LAMP2A

The crosslinked products between LAMP2A-FLAG and LAMP2A-MYC should be detected with both anti-FLAG and anti-MYC antibodies. Consistently, the crosslinked products detected with an anti-MYC antibody (Figure 2C) were detected with an anti-FLAG antibody (Figure 2D). However, to our surprise, the crosslinked products with LAMP2A-FLAG<sup>P261X</sup> or LAMP2A-FLAG<sup>R278X</sup> (X: *p*Bpa) were quite strongly detected with the anti-FLAG antibody (Figure 2D), and thus these *p*Bpa-containing variants of LAMP2A-FLAG may preferentially crosslink with each other.

In order to examine this possibility, the crosslinker amino acid was introduced in place of P261 in two ways for comparison (Figure 3). When *p*Bpa was introduced only in LAMP2A-FLAG<sup>P261X</sup> (X: *p*Bpa) (Figure 3A), the crosslinked products were detected much more prominently with the anti-FLAG antibody than with the anti-MYC antibody (Figure 3C, lanes 1 and 2), similarly to the results in Figure 2C,D. On the other hand, when *p*Bpa was introduced to both LAMP2A-FLAG<sup>P261X</sup> and LAMP2A-MYC<sup>P261X</sup> (X: *p*Bpa) (Figure 3B), the crosslinked products were clearly detected with both anti-FLAG and anti-MYC antibodies (Figure 3C, lanes 3 and 4). Therefore, the *p*Bpa-bearing variant LAMP2A molecules were crosslinked to each other more efficiently than to the LAMP2A molecules without *p*Bpa.

This observation indicated that the incorporation of *p*Bpa at this position potentiates the homophilic interaction of LAMP2A, leading to efficient crosslinking (Fig. S3A). Presumably, the size of the *p*Bpa side chain is just large enough to fill the space between the LAMP2A molecules, and the hydrophobic *p*-benzyl benzene moiety of *p*Bpa (Figure 2A) in one molecule directly interacts with the other molecule of LAMP2A. These results revealed that the LAMP2A molecules interact via side A of the C-domain. Presumably, the variants LAMP2A<sup>R278X</sup> (X: *p*Bpa) with *p*Bpa on side A were also crosslinked preferentially to each other.

The expression of a variant protein with a non-natural amino acid incorporated at the artificial UAG site, via the engineered tRNA and aminoacyl-tRNA synthetase pair, is generally lower than that of the wild-type protein. Thus, the association between variant proteins (“minor” and “minor”) might be disadvantageous, as compared to that between the variant protein and the wild-type protein (“minor” and “major”). Nevertheless, as described above, the LAMP2A<sup>P261X</sup> (or LAMP2A<sup>R278X</sup>) (X: *p*Bpa) variants interact with each other. The incorporation of *p*Bpa at positions other than P261 and R278 did not cause this effect, which suggested

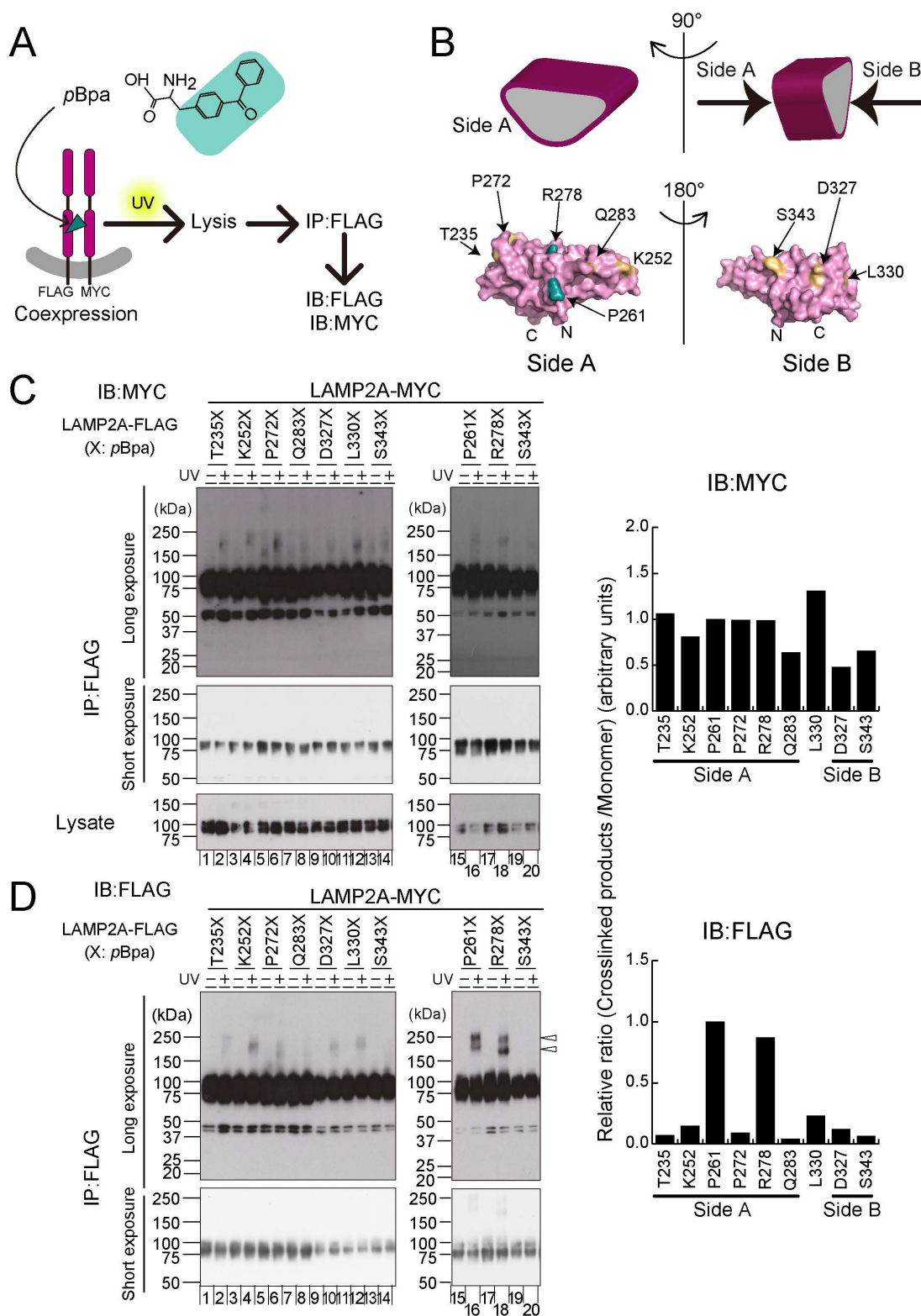


**Figure 2.** Direct homophilic interaction of mouse LAMP2A molecules in HEK293c18 cells revealed by site-specific crosslinking. (A) The chemical structure of pBpa (*p*-benzoyl-L-phenylalanine). The combination of the C-terminally FLAG-tagged and MYC-tagged LAMP2A proteins on the membrane is schematically shown. The triangle (green) shows the crosslinker. (B) Schematic  $\beta$ -prism shapes are shown in two perpendicular views. We defined the surface of the  $\beta$ -prism on the N-terminal side as Side A, and that on the C-terminal side as Side B. The crosslinker (pBpa) was introduced into the residues in the C-domain of mouse LAMP2A, and are superimposed on those of the C-domain of mouse LAMP1 (208–370) in two inverted views (PDB 5GV0). N: N terminus of the C-domain; C: C terminus of the C-domain. (C, D) HEK293c18 cells were transfected with the amber mutant of FLAG-tagged LAMP2A and the wild-type MYC-tagged LAMP2A. After light-dependent crosslinking, the reactions were analyzed by immunoblotting. Open triangles in (D) show the presence of two bands, in the cases of LAMP2A<sup>P261X</sup> and LAMP2A<sup>R278X</sup> (X: pBpa). The band intensities were analyzed as described in the Materials and Methods. The results obtained from the left and right panels in (C and D) were integrated, using the value for LAMP2A<sup>S343X</sup> (X: pBpa). Essentially the same results were obtained in an independent experiment. See also Fig. S3.

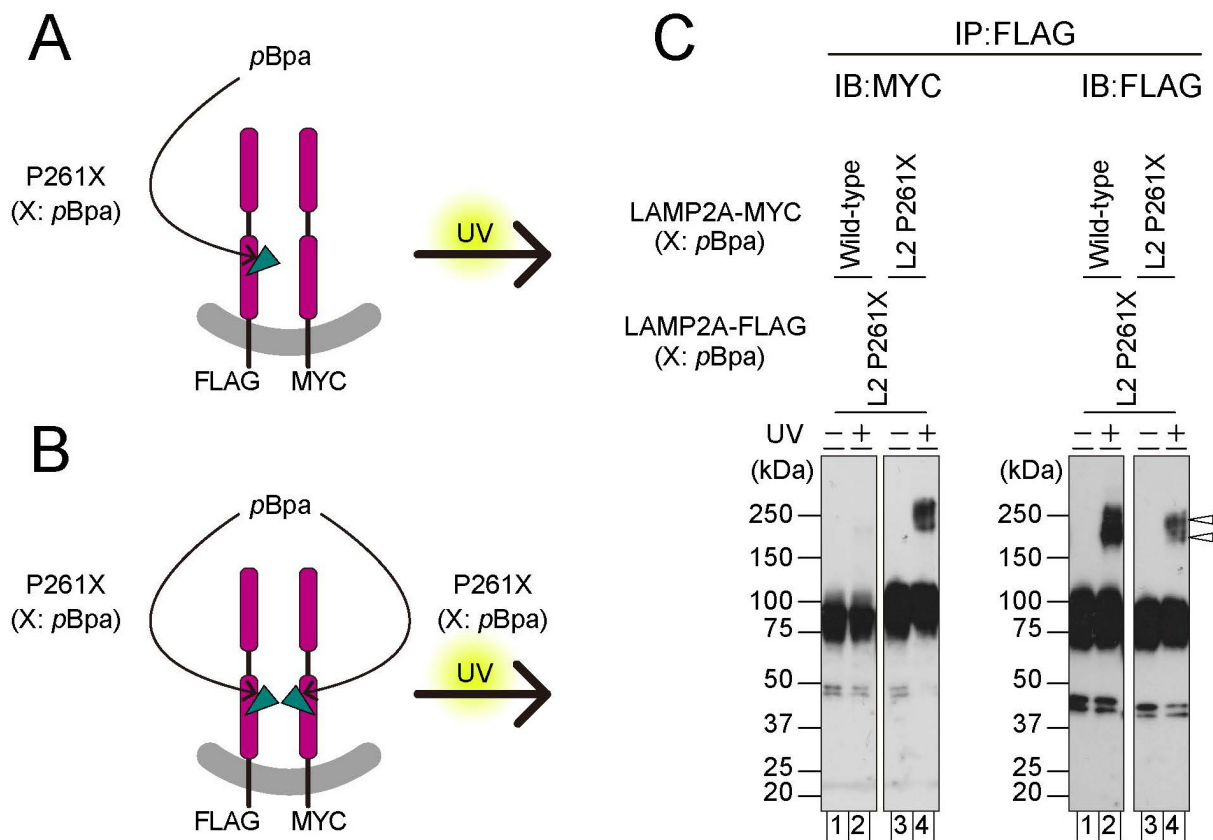


**Figure 3.** The mouse LAMP2A protein variants with *pBpa* in place of P261 crosslink each other. (A, B) The crosslinker (*pBpa*) was introduced to either the amber mutant of FLAG-tagged LAMP2A (A), or both amber mutants of FLAG-tagged LAMP2A and MYC-tagged LAMP2A (B). (C) After light-dependent crosslinking, the reactions were analyzed by immunoblotting. Open triangles show the presence of two bands. Essentially the same results were obtained in an independent experiment.

that P261 and R278 are located at crucial positions for the side-A-facing homophilic interaction of LAMP2A (Fig. S3B). Because the crosslinked products appeared as two bands (Figure 2D, 3C, open triangles), there should be at least two different crosslinking modes.

#### The *pBpa*-dependent crosslinking at P261 and R278 occurs even in heavily glycosylated polypeptide regions

The LAMP family proteins are heavily glycosylated. There are nine potential *N*-linked glycosylation sites in the C-domain of LAMP2A (Fig. S1C). Among them, N227 is ~10 Å away from P261, while N265 and N280 are ~5 Å away from R278 (Figure 4A). To examine whether the *N*-linked oligosaccharide moieties attached to these residues on side A are involved in the *pBpa*-dependent crosslinking, we treated the crosslinked products with PNGaseF, to remove the *N*-linked oligosaccharide moieties from LAMP2A (Figure 4B). If *pBpa* only reacted with the oligosaccharide moieties, then detaching these moieties from LAMP2A would resolve the crosslinked products into a monomeric form. On the other hand, if the polypeptide moieties were crosslinked with each other, then detaching the oligosaccharides would not affect the covalently bonded assembly of LAMP2A, and

the crosslinked product would migrate more slowly than monomeric LAMP2A even after the PNGaseF treatment.

As shown in Figure 4C, the molecular mass of the LAMP2A monomers decreased upon the PNGaseF treatment, from at around 100 kDa to ~50 kDa, as expected. The crosslinked products after the PNGaseF treatment were detected with an anti-MYC antibody at 130 kDa (Figure 4C, left, lanes 4 and 8) and with an anti-FLAG antibody at 160 and 130 kDa (Figure 4C, right, lanes 4 and 8 with *pBpa* in place of P261 and R278, respectively). Accordingly, *pBpa* at P261 or R278 reacted with the polypeptide moieties of LAMP2A, despite the presence of many *N*-linked oligosaccharide moieties.

Before the PNGaseF treatment, LAMP2A-FLAG<sup>P261X</sup> (X: *pBpa*) gave rise to two crosslinked products at around 180 and 250 kDa and the monomers at 110 and 90 kDa, as detected with an anti-FLAG antibody (Figure 4C, right, lane 3). As described above, two crosslinked products were also observed in Figures 2D and 3C. After the PNGaseF treatment, the crosslinked products of the deglycosylated LAMP2-FLAG were observed at 160 and 130 kDa (Figure 4C, right, lane 4), along with the monomers at 55 and 45 kDa. The two species were probably due to the different extents of the oligosaccharide moiety removal (Figure 4C, right). The sizes of the crosslinked products and monomers after the PNGaseF treatment

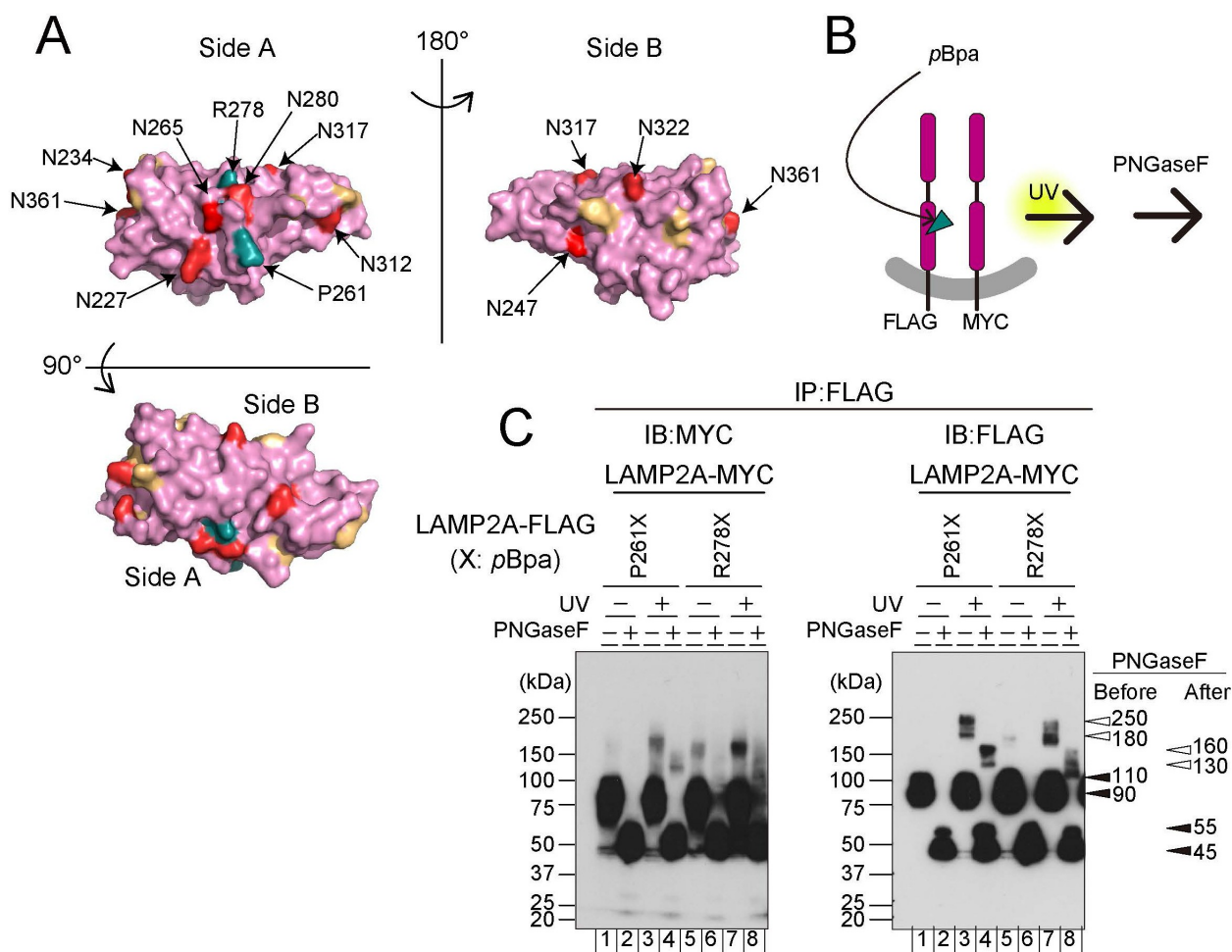


**Figure 4.** The crosslinked product of mouse LAMP2A<sup>P261X</sup> or LAMP2A<sup>R278X</sup> (X: pBpa) was observed even after the PNGaseF treatment. (A) The putative N-glycosylation sites in the C-domain of LAMP2A are shown in the C-domain of LAMP1 (5GV0), in two inverted views and two perpendicular views (red). The residues to which the crosslinker was introduced in Figure 2 are also shown in yellow and green (P261 and R278). (B) HEK293c18 cells were transfected with mouse LAMP2A-FLAG<sup>P261X</sup> or LAMP2A-FLAG<sup>R278X</sup> (X: pBpa), and the wild-type MYC-tagged mouse LAMP2A. (C) After light-dependent crosslinking, the samples were subjected to the PNGaseF treatment as described in the Materials and Methods and the reactions were analyzed by immunoblotting. The sizes of the crosslinked products (open triangles) and monomers (closed triangles) of LAMP2A<sup>P261X</sup> (X: pBpa) before and after the PNGaseF treatment are shown in kDa. Essentially the same results were obtained in an independent experiment.

suggested the presence of dimeric and trimeric assemblies of the variant LAMP2A.

#### Direct homophilic interactions of human LAMP2A revealed by site-specific crosslinking

Since the amino acid sequence homology within the C-domains of mouse and human LAMP2A is as high as 75% (Fig. S3C), we introduced pBpa into K247, P256, and R273 in human LAMP2A, which correspond to K252, P261, and R278 in mouse LAMP2A, respectively (Fig. S3D). The crosslinked products of the human LAMP2A-FLAG<sup>K247X</sup>, LAMP2A-FLAG<sup>P256X</sup> and LAMP2A-FLAG<sup>R273X</sup> (X: pBpa) were clearly detected with both the anti-MYC and anti-FLAG antibodies, revealing the direct homophilic interactions of human LAMP2A (Figs. S3E, F). The crosslinking at K247 in human LAMP2A (Figs. S3E, F) is more efficient than that at K252 in mouse LAMP2A (Figure 2D). The other crosslinking sites will be evaluated in future studies.

#### Hydrophilic replacement of T235 or Q283 in LAMP2A affects its homophilic interaction, supporting the side-A-facing interaction

As described above, P261 and R278 are close to the region where the direct homophilic interaction of mouse LAMP2A occurs, and the incorporations of pBpa at these positions strengthened the homophilic interaction. The side chain of pBpa is longer than those of Pro and Arg, and thus the phenyl group at the tip of the pBpa side chain of one LAMP2A molecule could reach the other LAMP2A molecule. In order to examine whether S282 or Q283 on side A, residing 11 ~ 13 Å away from P261 and R278, is involved in the homophilic interaction, we generated LAMP2A-MYC<sup>S282E</sup> and LAMP2A-MYC<sup>Q283E</sup> and analyzed the immunoprecipitation efficiencies with retrieval by the wild-type LAMP2A-FLAG (Fig. S4A). As references, LAMP2A-MYC<sup>R346E</sup> and LAMP2A-MYC<sup>S343E</sup> were generated. The immunoprecipitation efficiencies of the four variants were not decreased (Fig. S4B). Instead, the immunoprecipitation efficiency was slightly



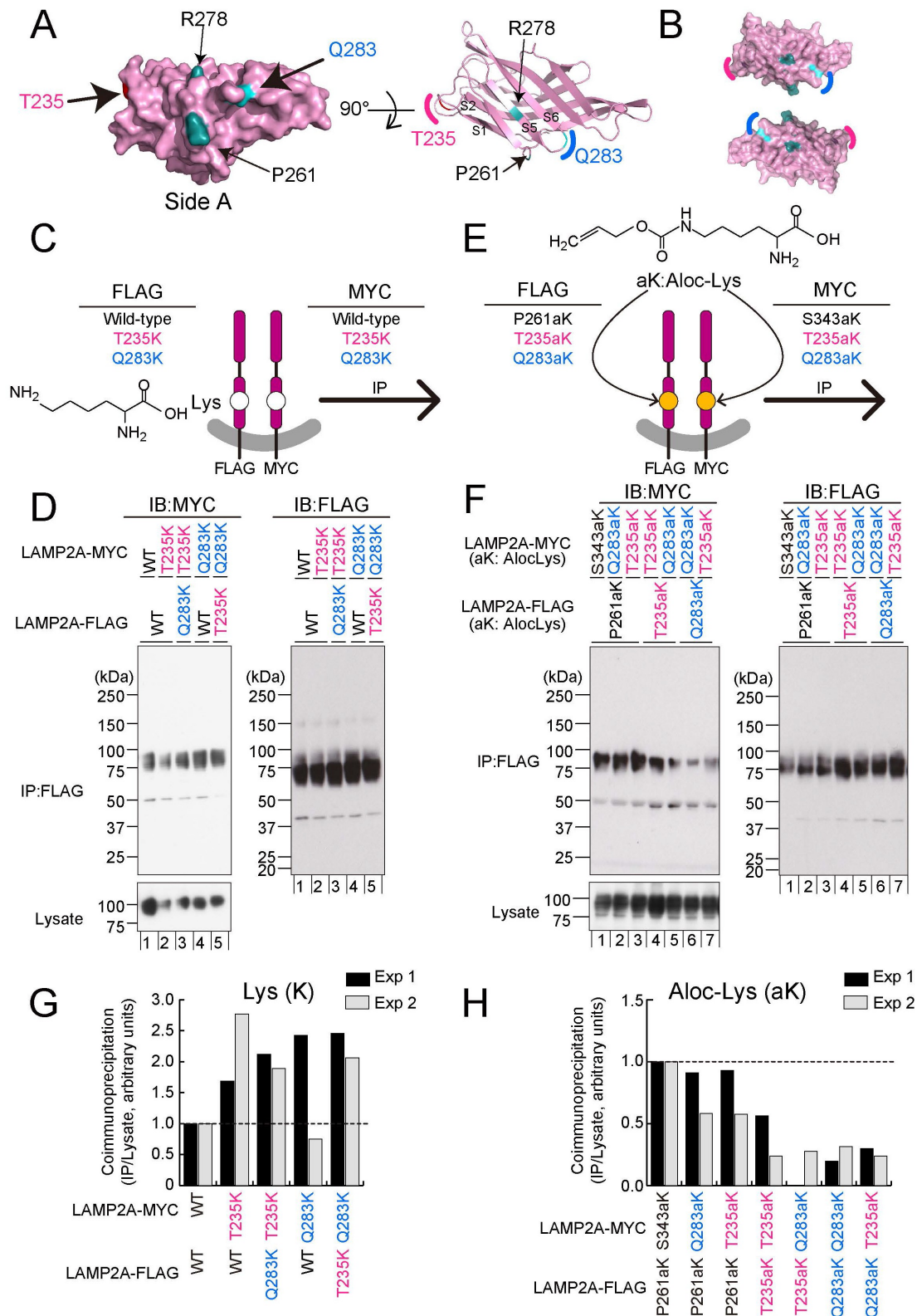


**Figure 5.** Disruption of the homophilic interaction of mouse LAMP2A by Aloc-Lys incorporation at T235 or Q283 in either member of the LAMP2A pair. (A) In addition to P261 and R278, T235 (pink) and Q283 (blue) are superimposed on those residues in the C-domain of mouse LAMP1 (208–370) in two perpendicular views (PDB 5GV0). The  $\beta$ -strand numbers (as indicated in Fig. S1C) are shown (S1, S2, S5, S6). (B) Locations of T235 and Q283 in the C-domains of two LAMP2A molecules with side A facing inward. (C) The wild-type, LAMP2A-FLAG<sup>T235K</sup> or LAMP2A-FLAG<sup>Q283K</sup> was coexpressed with the wild-type, LAMP2A-MYC<sup>T235K</sup> or LAMP2A-MYC<sup>Q283K</sup> in HEK293c18 cells. The amounts of MYC-tagged LAMP2A coimmunoprecipitated with FLAG-tagged LAMP2A in different combinations were then compared. (D) The lysate was subjected to immunoprecipitation with an anti-FLAG-antibody and analyzed by immunoblotting. (E) LAMP2A-FLAG<sup>P261aK</sup>, LAMP2A-FLAG<sup>T235aK</sup> or LAMP2A-FLAG<sup>Q283aK</sup> (aK: Aloc-Lys) was coexpressed with LAMP2A-MYC<sup>S343aK</sup>, LAMP2A-MYC<sup>T235aK</sup> or LAMP2A-MYC<sup>Q283aK</sup> (aK: Aloc-Lys) in HEK293c18 cells. The incorporation of Aloc-Lys was performed as described in the Materials and Methods. The amounts of MYC-tagged LAMP2A coimmunoprecipitated with FLAG-tagged LAMP2A in different combinations were then compared. The chemical structure of Aloc-Lys (N- $\epsilon$ -allyloxycarbonyl-L-lysine). (F) The lysate was subjected to immunoprecipitation with an anti-FLAG-antibody and analyzed by immunoblotting. (G, H) The band intensities of the immunoprecipitates (D, F, respectively) were normalized with those of the corresponding lysate. The results in (D, F) and those obtained in an independent experiment (black and gray, respectively) are shown after standardization, using the value obtained for the combination of the wild-type (Lys mutant) or S343 and P261 variant pair (Aloc-Lys mutant). aK, Aloc-Lys. See also Fig. S4.

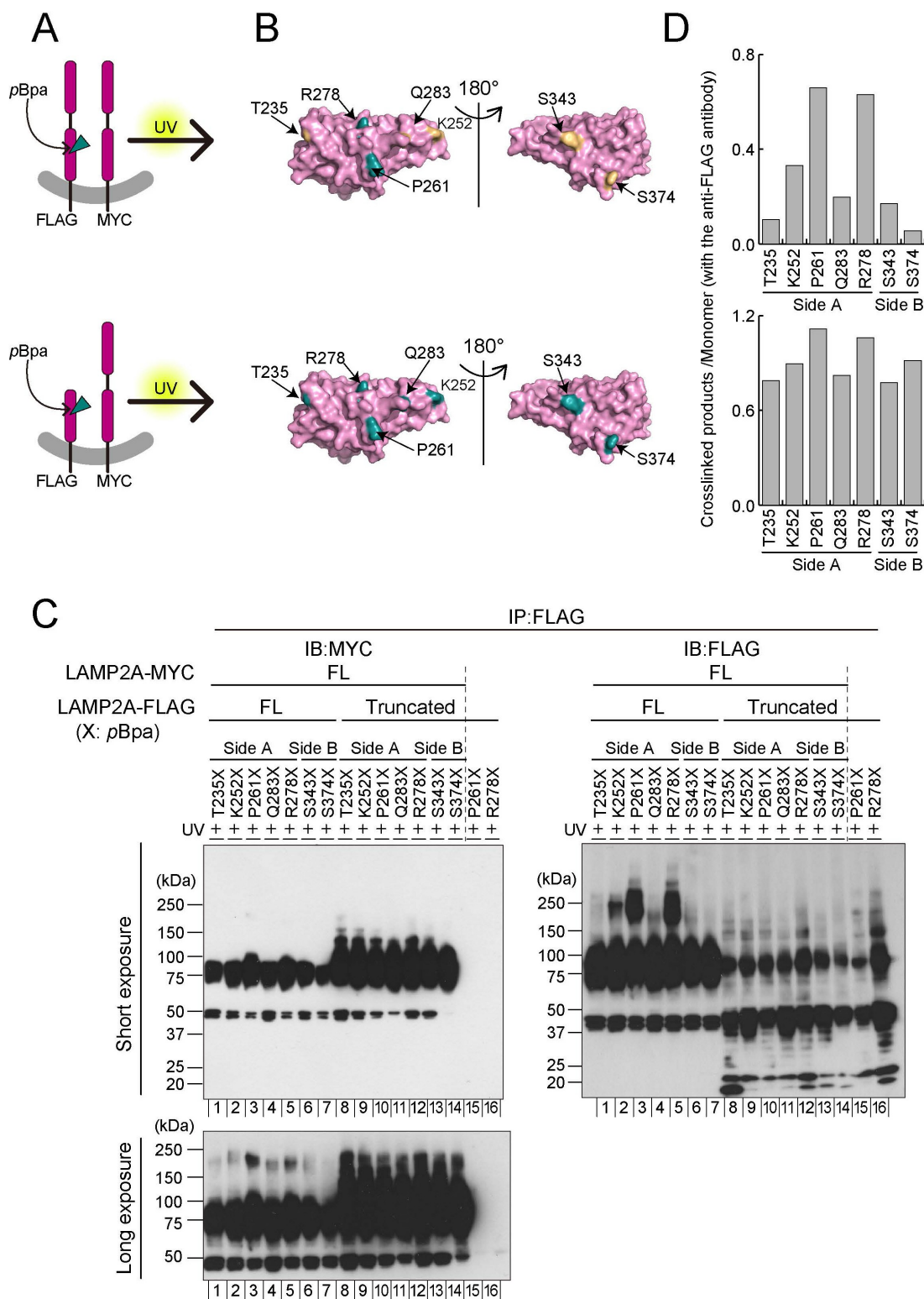


**Figure 6.** The N-domain truncation of mouse LAMP2A impairs the side A-specific homophilic interaction. (A) Comparison of the two situations. The crosslinker ( $pBpa$ ) was introduced into the residues in the C-domain of either the full-length or N-domain truncated mouse LAMP2A. (B) The residues with appreciable crosslinking are shown in blue, and are superimposed on those of the C-domain of mouse LAMP1 (208–370) in two inverted views (PDB 5GV0). (C) HEK293c18 cells were transfected with the amber mutants of the full-length (lanes 1–7) or N-domain truncated (lanes 8–16) FLAG-tagged LAMP2A and the wild-type MYC-tagged LAMP2A (lanes 1–14). After light-dependent crosslinking, the samples were analyzed by immunoblotting. Essentially the same results were obtained in an independent experiment. (D) The band intensities were analyzed as described in the Materials and Methods. See also Fig. S5.

increased in the case of LAMP2A<sup>Q283E</sup>, suggesting that the hydrophilic interaction of the side chain of residue 283 is enhanced by this mutation. Considering the similar sizes of

the Gln and Glu side chains, the original side chain of Q283 could be quite close to the other LAMP2A molecule.

The Q283 residue is located on the loop connecting  $\beta$ -strands S5 and S6 (Figure 5A). In the side-A-faced model structure, the loop connecting S5 and S6 interacts with the loop connecting S1 and S2 (Figure 5B). In order to test its importance, as well as that of T235, we generated LAMP2A-FLAG<sup>Q283K</sup>, LAMP2A-FLAG<sup>T235K</sup>, LAMP2A-MYC<sup>Q283K</sup> and LAMP2A-MYC<sup>T235K</sup> with a single mutation at either Q283 or T235 (on the loop connecting S1 and S2) to positively charged Lys and analyzed the immunoprecipitation efficiencies of their combinations (Figure 5C). Both mutations, Q283K and T235K, increased the coimmunoprecipitation efficiency (Figure 5D,G), suggesting that Q283 and T235 are located at important positions for the homophilic interaction of LAMP2A. Therefore, Q283 and T235 of one molecule are both close to the other molecule in the homophilic interaction, consequently supporting the side-A-faced interaction.

### **Steric hindrance at T235 or Q283 in LAMP2A by replacement with a lysine derivative impairs its homophilic interaction, supporting the side-A-facing interaction**

To further examine how close Q283 and/or T235 are to the other LAMP2A molecule in the homophilic interaction, we introduced a non-natural amino acid, N<sup>ε</sup>-allyloxycarbonyl-L-lysine (Aloc-Lys), which is bulkier and 6 Å longer than Lys (Figure 5E, Fig. S4C), by the expanded genetic code. Aloc-Lys (referred to as aK in Figure 5E, F, H) was introduced to the variant LAMP2A at the position mutated to the *amber* codon, during translation with a natural amber suppressor (tRNA<sup>Pyl</sup>) and the engineered pyrrolysyl-tRNA synthetase pair [37]. The expression levels of LAMP2A-MYC<sup>Q283aK</sup>, LAMP2A-MYC<sup>T235aK</sup>, LAMP2A-FLAG<sup>P261aK</sup>, and LAMP2A-MYC<sup>Q283aK</sup> (aK: Aloc-Lys) were comparable (Figure 5F). Nonetheless, the immunoprecipitation efficiencies of LAMP2A-MYC<sup>Q283aK</sup> and LAMP2A-MYC<sup>T235aK</sup> were lower than that of LAMP2A-MYC<sup>Q283aK</sup>, when retrieved by LAMP2A-FLAG<sup>P261aK</sup> (aK: Aloc-Lys). In addition, the amounts of immunoprecipitated LAMP2A-MYC<sup>Q283aK</sup> and LAMP2A-MYC<sup>T235aK</sup> were further reduced when retrieved by LAMP2A-FLAG<sup>Q283aK</sup> or LAMP2A-FLAG<sup>T235aK</sup> (aK: Aloc-Lys) (Figure 5F,H). These results indicated that the incorporation of Aloc-Lys at these positions causes steric hindrance with the other molecule, and thereby impairs the homophilic interaction (Fig. S4C). Thus, the distances between the two LAMP2A molecules in the homophilic interaction are shorter than those required for Aloc-Lys, but suitable for Lys accommodation at positions 283 and 235.

Accordingly, these mutation analyses (Figure 5), together with the crosslinking of the LAMP2A variants with pBpa in place of P261 and R278 (Figures 2 and 3), demonstrated that the side-A-facing geometry plays an important role in the assembly of LAMP2A.

### **The N-domain restricts the homophilic interaction of LAMP2A to be side A-specific**

In the next step, we investigated the effect of the N-domain truncation on the side-A-faced homophilic interaction of

LAMP2A. For this purpose, we compared the crosslinking of the full-length and N-domain-truncated variants bearing pBpa in the C-domain of LAMP2A-FLAG with the full-length LAMP2A-MYC (Figure 6A,B).

By immunoblotting with the anti-MYC antibody, consistent with our previous study [4], the amount of LAMP2A-MYC that coimmunoprecipitated with the truncated LAMP2A-FLAG was more than that obtained with the full-length LAMP2A-FLAG (Figure 6C, left panels, lanes 1–7 vs. 8–14). More crosslinked products were detected between the truncated LAMP2A-FLAG and LAMP2A-MYC than between the full-length LAMP2A-FLAG and LAMP2A-MYC. The crosslinked products of the truncated LAMP2A-FLAG variant (~200 kDa) were observed, regardless of whether pBpa was incorporated into side A (T235, K252, P261, R278, Q283) or side B (S343 and S374) of the  $\beta$ -prism of the C-domain (Figure 6C, left panels, lanes 8–14 after long exposure).

By immunoblotting with the anti-FLAG antibody, the crosslinked products of the full-length LAMP2A-FLAG<sup>P261X</sup> or LAMP2A-FLAG<sup>R278X</sup> variants (X: pBpa) were prominently observed, as compared to those of LAMP2A-FLAG<sup>T235X</sup>, LAMP2A-FLAG<sup>K252X</sup>, LAMP2A-FLAG<sup>Q283X</sup>, LAMP2A-FLAG<sup>S343X</sup>, or LAMP2A-FLAG<sup>S374X</sup> (X: pBpa) (Figure 6C, right panel, lanes 1–7). The crosslinked products of LAMP2A-FLAG<sup>P261X</sup> or LAMP2A-FLAG<sup>R278X</sup> (X: pBpa) were likely due to mutual crosslinking, based on the result in Figure 3. In the case of the truncated LAMP2A-FLAG variant, as shown in Figure 6C, right panel, lanes 8–14, the crosslinked products were observed at 100 kDa, and were smaller than those detected with the anti-MYC antibody (~150 kDa or ~200 kDa after short or long exposure, respectively, Figure 6C, left panels). Since the crosslinked product of the truncated LAMP2A-FLAG variants was approximately twice as large as that of the monomer (~50 kDa), these results implied that the truncated LAMP2A-FLAG variants are mutually crosslinked. However, in sharp contrast to the products of the full-length LAMP2A variants, those of the truncated LAMP2A-FLAG variants were observed regardless of whether the pBpa was incorporated into side A or side B. Considering these results, the side-A-specificity is apparently lost by the N-domain truncation (Figure 6D).

In the absence of the full-length LAMP2A-MYC, the truncated LAMP2A-FLAG<sup>R278X</sup> (X: pBpa) revealed a ladder (Figure 6C, right panel, lanes 15 and 16). This result suggested that more than three molecules of the truncated LAMP2A-FLAG<sup>R278X</sup> (X: pBpa) can be successively crosslinked. Although the efficient crosslinking of the full-length LAMP2A-FLAG<sup>P261X</sup> and LAMP2A-FLAG<sup>R278X</sup> (X: pBpa) occurred (Figure 6C, right panel, lanes 3 and 5), the ladder was less prominent in the case of the truncated LAMP2A-FLAG<sup>P261X</sup> (X: pBpa). Therefore, the presence or absence of the N-domain alters the manner of the homophilic association of LAMP2A.

Taken together, these results indicate that the truncation of the N-domain permits other homophilic interactions of LAMP2A that are not restricted to side A, and apparently strengthens the homophilic interaction. Accordingly, the N-domain restricts the homophilic interaction of LAMP2A to be side A-specific.

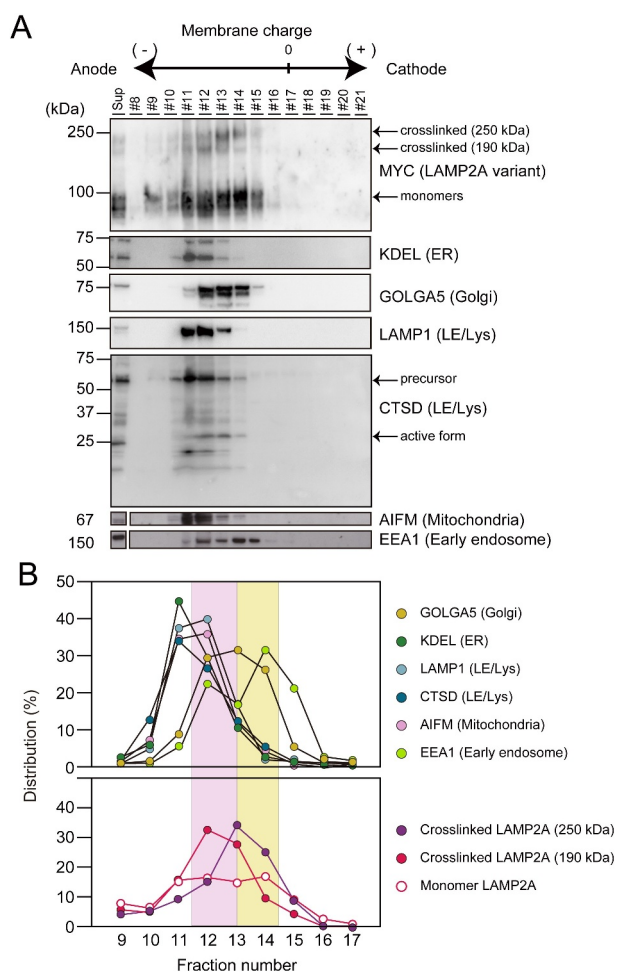


**Figure 7.** A portion of the crosslinked mouse LAMP2A is recovered in the same fractions containing the Golgi marker after subcellular fractionation by FFE. (A) HEK293c18 cells were transfected with the amber mutant of MYC-tagged mouse LAMP2A. After photo-crosslinking and cell disruption, the homogenate was separated by FFE, as described in the Materials and Methods, and analyzed by immunoblotting. (B) The distribution of each protein is expressed as the ratio to the sum of the intensities in #9 to #17.

### Interactions of the N-domains in the homophilic interaction of LAMP2A molecules

The N-domain is connected to the N terminus of the C-domain via the linker region (Fig. S5A). When we introduced *pBpa* in the N-domain of the variant LAMP2A-FLAG (Fig. S5B), the crosslinking was influenced by the presence/absence of the N-domain in LAMP2A-MYC (Figs. S5C, D), potentially implying the interaction between the N-domains, as follows. The crosslinked products between the truncated LAMP2A-MYC and LAMP2A-FLAG<sup>K58X</sup> or LAMP2A-FLAG<sup>D118X</sup> (X: *pBpa*) were more abundant than those with LAMP2A-FLAG<sup>T53X</sup>, LAMP2A-FLAG<sup>L143X</sup>, LAMP2A-FLAG<sup>L157X</sup>, LAMP2A-FLAG<sup>E186X</sup> or LAMP2A-FLAG<sup>M85X</sup> (X: *pBpa*) (Fig. S5E, left panel, lanes 2 and 3 versus lanes 1 and 4–7, respectively). On the other hand, the amounts of the crosslinked products between the full-length LAMP2A-MYC and LAMP2A-FLAG<sup>K58X</sup>, LAMP2A-FLAG<sup>L157X</sup> or LAMP2A-FLAG<sup>M85X</sup> (X: *pBpa*) were comparable (Fig. S5E, left panel, lanes 8–10). These results raised the possibility

that L157 and M85 are involved in an interaction between the N-domains, which should be verified in a future study. Therefore, the N-domain restricts the homophilic interaction of LAMP2A to be side A-specific, probably through the putative homophilic interactions.

On the other hand, we did not observe any appreciable amounts of crosslinked products with an anti-FLAG antibody (Fig. S5E, right panel). Thus, the LAMP2A-FLAG variants with *pBpa* in the N-domain probably did not preferentially crosslink with each other.

### LAMP2A is assembled before exiting from the Golgi apparatus

The photo-crosslinking reaction proceeds wherever the LAMP2A variant is present within the cell. Thus, in every process of its biosynthetic pathway, LAMP2A can theoretically be crosslinked. To investigate whether LAMP2A is assembled before arriving at acidic compartments, the crosslinked products were analyzed after subcellular fractionation. The LAMP2A-MYC<sup>P261X</sup> (X: *pBpa*) variant was transiently expressed in HEK293c18 cells. After UV irradiation, the cells were disrupted by nitrogen cavitation, and the subcellular organelles were separated by free-flow electrophoresis (FFE) [38,39]. As shown in Figure 7, LE/Lys (LAMP1 and CTSD), ER (KDEL) and mitochondria (AIFM) were recovered within the same anodally deflected fractions, whereas the Golgi apparatus (GOLGA5) and early endosomes (EEA1) were within the less deflected fractions. LAMP2A-MYC<sup>P261X</sup> (X: *pBpa*) gave rise to two crosslinked products at around 190 and 250 kDa. The former product (190 kDa) was recovered within the fractions containing ER, LE/Lys, mitochondria and the Golgi apparatus, while the latter products (250 kDa) were recovered mainly with the Golgi apparatus. These results suggested that some parts of LAMP2A-M<sup>P261X</sup> (X: *pBpa*) are assembled within the Golgi apparatus, before arriving at acidic compartments.

### Variant mouse LAMP1 proteins with *pBpa* in place of P251, relevant to P261 in mouse LAMP2A, crosslink each other

In our previous study, we noticed a smear in the high-molecular weight region of the mouse LAMP1 immunoblots, which was not observed in the mouse LAMP2 immunoblots [4]. As shown in Fig. S6A, the smear was appreciably relieved with reductive alkylation, suggesting a substantial difference between the assembly modes of mouse LAMP1 and LAMP2.

To compare the homophilic interaction of the C-domain of LAMP1 with that of LAMP2A, the crosslinker was introduced into the C-domain of LAMP1 at the positions corresponding to those in the case of LAMP2A, and the proteins were analyzed in a crosslinking experiment (Figure 8A). The crosslinked products between the variant LAMP1-FLAG and LAMP1-MYC were observed with the anti-MYC antibody, indicating that the C-domain contributes to the homophilic interaction of mouse LAMP1 (Figure 8B, left panel).

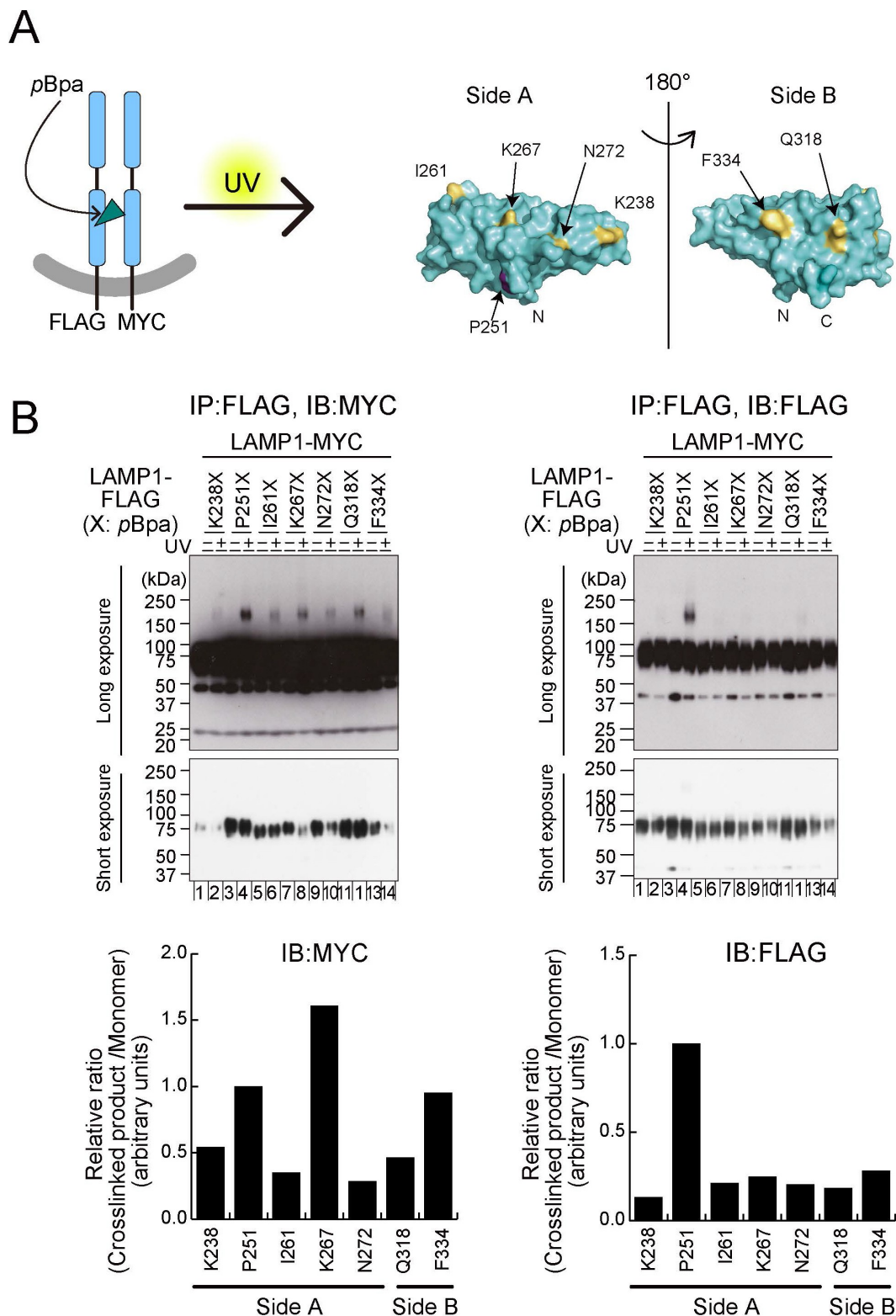


**Figure 8.** Homophilic interaction of mouse LAMP1 molecules in HEK293c18 cells revealed by site-specific crosslinking. (A) The crosslinker ( $\rho$ Bpa) was introduced into the residues in the C-domain of mouse LAMP1, which are superimposed on those of the C-domain of mouse LAMP1 (208–370) in two inverted views (PDB 5GV0). (B) HEK293c18 cells were transfected with the amber mutant of FLAG-tagged LAMP1 and wild-type MYC-tagged LAMP1. After light-dependent crosslinking, the samples were subjected to reductive alkylation and analyzed by immunoblotting. The band intensities were analyzed as described in the Materials and Methods. Essentially the same results were obtained in an independent experiment. See also Fig. S6.

The anti-FLAG immunoblot revealed prominent crosslinking for LAMP1-FLAG<sup>P251X</sup>, which corresponds to LAMP2A-FLAG<sup>P261X</sup> (X:  $\rho$ Bpa) (Figure 8B, right panel, lanes 3 and 4). As in the case of LAMP2A (Figure 3A), the crosslinker was introduced to only LAMP1-FLAG<sup>P251X</sup> or to both LAMP1-

FLAG<sup>P251X</sup> and LAMP1-MYC<sup>P251X</sup> (X:  $\rho$ Bpa) (Fig. S6B, C, respectively). In the latter case, the crosslinked products were clearly detected with both anti-FLAG and anti-MYC antibodies (Fig. S6D, lanes 3 and 4), indicating that the LAMP1<sup>P251X</sup> (X:  $\rho$ Bpa) proteins were mutually crosslinked.

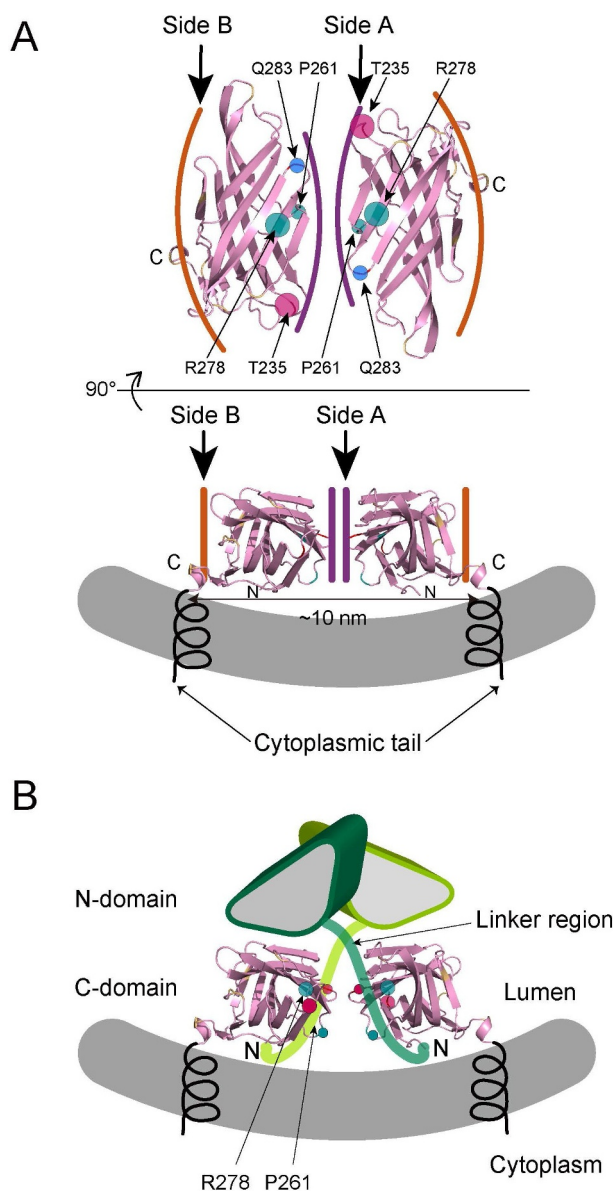


**Figure 9.** Schematic representation of the homophilic interaction of mouse LAMP2A on the luminal membrane. (A) The C-domains of two LAMP2A proteins in the side-A-faced orientation in two perpendicular views. The residues corresponding to P261 and R278, to which the incorporation of *pBpa* results in efficient crosslinking, are shown in small and large green circles, respectively. The residues corresponding to T235 and Q283, to which the incorporation of Aloc-Lys impaired the homophilic interaction, are shown in large red and small blue circles, respectively. The structure is that of the C-domain of mouse LAMP1 (PDB 5GV0). Purple and orange curves show the positions of side A and side B, respectively. N: N terminus of the C-domain. C: C terminus of the C-domain. (B) Schematic representation of the dimeric interactions of full-length LAMP2A on the luminal membrane. The N-domains attached to the C-domain on the left and the right are shown in yellowish green and deep green circles, respectively. See also Fig. S7.

However, unlike the case of mouse LAMP2A, the crosslinked product of LAMP1<sup>K267X</sup>, corresponding to LAMP2<sup>R278X</sup> (X: *pBpa*), was not detected with the anti-FLAG antibody (Figure 8B, right panel, lanes 7 and 8). Therefore, although side A of the C-domain of LAMP1 is involved in the homophilic interaction between LAMP1 proteins, the assembly mode of LAMP1 is different from that of LAMP2A.

## Discussion

The present study is the first to reveal the direct homophilic interaction of mouse LAMP2A molecules within cells, as determined by using expanded genetic code technologies.

The results demonstrated that the LAMP2A molecules on the luminal membrane face each side A of the  $\beta$ -prism of the C-domain toward the other. On the other hand, the truncated LAMP2A lacking the N-domain and the linker region assembled on both sides of the  $\beta$ -prism of the C-domains. Thus, although the presence of the N-domain apparently weakened the homophilic interaction of LAMP2A, as in our previous immunoprecipitation study [4], the present study renewed the viewpoint that the two-domain structure restricts the homophilic interaction of LAMP2A to be side A-specific. Our results revealed that the N-domain truncation of LAMP2A impaired the recruitment of GAPDH-HT to the LE/Lys surface during the CMA process. In

addition, the truncation of LAMP2A affected the process of LE/Lys generation. Combining these results, we conclude that the two-domain architecture is important for the functional aspects of mouse LAMP2A. We will discuss below how the two-domain architecture is required to form the specific homophilic interactions of LAMP2A and how the interactions of the luminal domains control the function of LAMP2A.

The linker region of mouse LAMP2A is composed of 33 amino acid residues, containing eight proline residues and eighteen potential *O*-glycosylation sites (Fig. S1C). Thus, the linker region is likely to be elongated and rigid after *O*-glycosylation. The length of the linker region of mouse LAMP2A is estimated to be approximately 10 nm, based on the previous simulation of the human LAMP1 linker region (PSPTTAPPAPPSPSPSP, 17 amino acid residues) starting from the initial structure carrying *O*-glycans on the six Ser/Thr residues, which was 5 nm [5]. In our model, the N terminus of the C-domain, where the linker region is attached, is located near the luminal membrane (Figure 9A). We propose that the linker region is perpendicular to the membrane along the C-domain, which restricts the interaction between the N-domains to the side-A-faced arrangement of the C-domains (Figure 9B). In order to characterize the assembly modes definitively, a new approach is still required to identify the crosslinked site on the other side of LAMP2A.

Our crosslinking experiments suggested the dimeric and trimeric assemblies (190 and 250 kDa, respectively) for LAMP2A<sup>P261X</sup> (X: pBpa). Both assemblies are possible, in which side A faces in an antiparallel manner and at 120 degrees, respectively (Fig. S7). It should be noted that the trimeric crosslinked product at 250 kDa was distributed within the Golgi apparatus fractions in the subcellular fractionation by FFE. The result raised the possibility that the glycosylation of LAMP2A within the Golgi apparatus, including the *O*-linked glycosylation of the linker region, is involved in regulating the trimeric interaction of LAMP2A.

The present study revealed the importance of the homophilic interaction of LAMP2A in the recruitment of GAPDH-HT to the surface of LE/Lys. The carboxyl termini of the two C-domains should be approximately 10 nm apart in the side-A-faced homophilic interactions, either dimeric or trimeric, of the full-length LAMP2A, and thus the cytoplasmic tails are also approximately 10 nm apart (Figure 9A, S7). However, in the case of the truncated LAMP2A, the distance between the cytoplasmic tails can be closer due to the interactions between sides A and B of the C-domains. Thus, the N-domain truncation affects the distance between the cytoplasmic tails. We found that the N-domain truncation of LAMP2A, with an intact C-terminal tail, reduced the recruitment of GAPDH-HT to the LE/Lys surface. Multiple molecules, such as GFAP [40] and MTORC2-PHLPP1-AKT [41], are recruited on the lysosome membrane in addition to the CMA substrates and chaperones/cochaperones during the course of CMA. It is conceivable that the proper arrangement of the cytoplasmic tails of LAMP2A on the lysosome membrane, defined by the side A-faced interactions of the luminal domains, would be a prerequisite for the effective binding of the CMA substrates,

chaperones and related molecules to form the translocation machinery.

A previous nuclear magnetic resonance (NMR) analysis revealed that the peptide containing the transmembrane domain and cytoplasmic tail of human LAMP2A (42 amino acid residues) forms a homotrimer in micelles [42]. The present LAMP2 assembly model itself is not compatible with the formation of the transmembrane domain homotrimer. However, if the assembled LAMP2 acts as a building unit in certain settings to form a larger structure, then the transmembrane domains could contact each other at the interfaces between the building units. Based on the present study, a strategy to isolate the CMA machinery, which maintains the side A-specific, homophilic interaction of LAMP2A, will be necessary to elucidate the mechanism of protein translocation across the lysosomal membrane.

Autophagic vacuoles reportedly accumulated in several tissues of LAMP2-deficient mice [8], as we also observed in LAMP2-deficient cultured cells [43]. Although the role of human LAMP2B in the autophagosome-lysosome fusion specifically in human cardiomyocytes was reported [12], the mechanism underlying the generation of abnormal vesicles in the absence of LAMP2A in other types of cells remains enigmatic. The present study suggested that the expression of the N-domain-truncated LAMP2A impaired the process of LE/Lys formation. Based on the present FFE study, some part of LAMP2A is probably assembled before arriving at an acidic compartment. Since the ER or Golgi apparatus is interconnected with late endosomes [44,45] and autophagosomes [46], the assembly of LAMP2A within the ER and/or Golgi apparatus may affect membrane-mediated events between these organelles and late endosomes and/or autophagosomes. It is possible that the homophilic interaction of LAMP2A contributes to the efficient recruitment of GAPDH-HT to the LE/Lys surface via the maturation of LE/Lys, in addition to the abovementioned possibility via the arrangement of the C-terminal tail of LAMP2A.

The LAMPs are abundant and heavily glycosylated proteins on lysosomal membranes, and were initially considered to function simply as a barrier, to protect the lysosomal membranes from the lytic environment by forming a glycocalyx. Consequently, the unique assembly modes of the LAMPs were unexpected. However, the present study revealed that mouse LAMP2A has its own unique assembly modes based on the two-domain architecture, thus paving the way toward understanding and manipulating the functions of LAMP2A.

## Materials and methods

### Cells and reagents

Mouse embryonic fibroblast cells from *rbc1cc1*-knockout mice (*rbc1cc1*<sup>-/-</sup> MEFs) [47] were maintained in DMEM (high glucose; Nacalai Tesque, 08458-16), supplemented with 10% fetal bovine serum (GIBCO, 260140-079). The human embryonic kidney cell line (HEK293c18) was obtained from

ATCC (CRL-10852). The HEK293c18 cells were seeded and maintained in growth media consisting of D-MEM/Ham's F12 (Wako, 048-29785), supplemented with 10% fetal bovine serum and 4 mM L-glutamine. All cells were maintained in the presence of L-penicillin (50 U/ml) and streptomycin (50 µg/ml) at 37°C in a 5% CO<sub>2</sub> atmosphere. pBpa (H00146; MW 269.3) and Aloc-Lys (M00517; MW 230.26) were obtained from Watanabe Chemical Industries (Hiroshima, Japan).

### Plasmids

The mouse *Lamp1* and *Lamp2a* cDNA clones in pCMV6-AC-GFP and the human *LAMP2*, transcript variant A, cDNA clone in pCMV6 were obtained from ORIGENE (MG225631, MG222878, and RC221216, respectively). The cDNAs encoding the full-length LAMP1 and LAMP2A molecules were amplified by PCR (*EcoRI-MluI* fragment) and subcloned into the pCEpuro vector [22]. The constructs were tagged with a triple FLAG epitope or a triple MYC epitope at the N or C terminus, or untagged. The stop codon was exchanged to an other codon. The resultant plasmids were used as templates to obtain the truncated LAMP2A. The LAMP2A gene in pCEpuro-mLAMP2A was mutagenized to create an amber codon, located at T53, K58, M85, D118, L143, L157, E186, T235, K252, P261, P272, R278, Q283, D327, L330, S343, or S374, and in pCEpuro-hLAMP2A at K247, P256, or R273. The LAMP1 gene in pCEpuro-mLAMP1 was mutagenized to create an amber codon located at K238, P251, I261, K267, N272, Q318, or F334. Site-directed mutagenesis (T235K, Q283K, T235K/Q283K) was performed with pCEpuro-mLAMP2A. Primers used in this study are listed in Table S1.

For the incorporation of pBpa or Aloc-Lys, pcpBpaRS ver.1, carrying the bacterial pair of an amber suppressor tRNA and an aminoacyl-tRNA synthase specific to pBpa [19], or the combination of pcPylRS<sup>Y384F/Y306A</sup> and pOriPpU6tRNA<sup>Pyl</sup> [20,48], was used.

The pcDNA5-GAPDH-HaloTag vector [26] was obtained from the RIKEN BioResource Research Center (RDB15088).

### Establishment of LAMP2-deficient cells

LAMP2-deficient *rbc1cc1*<sup>-/-</sup> MEFs were established by CRISPR-CAS9-mediated genome editing (*Lamp2*-mouse gene knockout kit via CRISPR, OriGene Technologies, KN309118) according to the manufacturer's protocol. The target sequences of guide RNA #1 (5' TTGCGCCTTTAACCGGAGAT 3') and guide RNA #2 (5' GAGGGCCCCGAAAACCTCACCT 3') were located near the 5' end of the ORF. After transfection of *rbc1cc1*<sup>-/-</sup> MEFs, knockout clones were isolated by limited dilution. The effective knock-out of *lamp2* was confirmed at the protein level by immunoblotting (Fig. S2A).

### Establishment of cells expressing N-terminally FLAG-tagged LAMP2A

LAMP2-deficient *rbc1cc1*<sup>-/-</sup> MEFs were transfected with the pCEpuro vector, carrying either the full-length or truncated, N-terminally FLAG-tagged mouse LAMP2A gene. After selection with 5 µg/ml puromycin, stable transfectants were isolated by limited dilution. The expression was confirmed at the protein level by immunoblotting.

### Transfectants stably expressing untagged or C-terminally FLAG-tagged mouse LAMP2A

LAMP2-deficient *rbc1cc1*<sup>-/-</sup> MEFs were transfected with the pCEpuro vector carrying either the full-length or truncated *Lamp2a* gene, which was either C-terminally FLAG-tagged or untagged. The puromycin (5 µg/ml)-resistant cells were used for immunocytochemistry.

### Observation of GAPDH-HT puncta formation

*rbc1cc1*<sup>-/-</sup> MEFs or LAMP2-deficient *rbc1cc1*<sup>-/-</sup> MEFs (1 x 10<sup>5</sup> cells/well) in a 12 well plate were cotransfected with either the pCEpuro plasmid or the N-terminally FLAG-tagged, full-length or N-domain truncated *Lamp2* gene (0.75 µg DNA) and GAPDH-HT (0.15 µg DNA), using the Avalanche-Everyday Transfection Reagent (EZ Biosystems, EZT-EVDY -1) (1 µl). The next day, the cells were incubated in culture medium containing 500 nM TMR-HT ligand (Promega, G8252) at 37°C for 10 min, followed by PBS (137 mM NaCl, 2.7 mM KCl, 10 mM NaH<sub>2</sub>PO<sub>4</sub>, 1.8 mM KH<sub>2</sub>PO<sub>4</sub>, pH 7.4) washes. The cells were then detached from the plate with a 0.05% trypsin solution, and half of the cells were seeded on poly-L-lysine-coated glass bottom dishes (Matsunami, D110310) and cultured further for 18 h.

For the quantitative evaluation of the puncta formation, live fluorescent images of GAPDH-HT were obtained by confocal microscopy, using an FV10iDOC microscope (Olympus, Tokyo, Japan). The images within a series of experiments were binarized using a common threshold and subjected to particle analysis with the Fiji software. The number of particles per cell was counted for those cells that contained at least one particle.

### Release of the 30 kDa protein from GAPDH-HT

*rbc1cc1*<sup>-/-</sup> MEFs or the stable transfectants, expressing either the N-terminally FLAG-tagged, full-length or truncated LAMP2A in LAMP2-deficient *rbc1cc1*<sup>-/-</sup> MEFs (2.5 x 10<sup>6</sup> cells), were transfected in 10 cm dishes without or with GAPDH-HT (10 µg DNA), using the Avalanche-Everyday Transfection Reagent (10 µl). The next day, the cells were incubated with culture medium containing 2 µM biotin-HT ligand (Promega, G8282) at 37°C for 30 min, washed with PBS and cultured further for 24 hours. The cells were then washed with PBS and lysed with 1% Triton X-100 (Sigma-Aldrich, T9284) in buffer A, consisting of 20 mM Tris-HCl,



pH 7.5, 150 mM NaCl, 10 mM iodoacetamide, 2.5 mM NaF, 2.5 mM sodium pyrophosphate, 10 mM ethylenediaminetetraacetic acid, 10 mM  $\beta$ -glycerophosphate, 1 mM sodium orthovanadate, 1 mM phenylmethylsulfonyl fluoride (Sigma-Aldrich, P7626), 5  $\mu$ g/ml leupeptin (PEPTIDE INSTITUTE, 4041), 10  $\mu$ g/ml pepstatin A (PEPTIDE INSTITUTE, 4397), and 10  $\mu$ g/ml aprotinin (Roche, 10 236 624 001). Cell lysates were incubated for 1 h at 4°C with Neutravidin beads (Pierce, 29200). After the resin was washed with buffer (50 mM Tris-HCl, pH 8.0, 150 mM NaCl, 5 mM EDTA, 0.5% Triton X-100, and 0.1% SDS), 60  $\mu$ l of SDS-sample buffer A, consisting of 750 mM Tris-HCl, pH 6.8, 20 mM dithiothreitol, 2.5% SDS, and 5% glycerol (w:v), was added to the resin. The resin was heated at 95°C for 5 min. After brief centrifugation, the materials eluted from the resin were analyzed by immunoblotting.

### Immunocytochemistry

The cells were cultured on 15-mm round glass coverslips coated with poly-L-lysine solution ( $\epsilon$ -poly-L-lysine coating solution; Cosmo Bio Co., Ltd. SPL01) in 12-well plates ( $5 \times 10^4$  cells/well). After 24 h, the cells were fixed with 4% paraformaldehyde (PFA) in PBS for 10 min, followed by permeabilization with 0.1% Triton X-100 in PBS containing 0.1 M glycine (Fig. S2B) for 5 min. In the experiments shown in Figs. S2G, H, J, and K, the cells were fixed with 3% paraformaldehyde (PFA) in PBS for 20 min and permeabilized with digitonin (50  $\mu$ g/ml; Wako, 043-21376) in PBS containing 0.1 M glycine for 5 min. The cells were then washed with PBS, blocked with 1% bovine serum albumin (BSA) in PBS for 30 min at RT, and then stained with the primary antibodies for 1 h at RT. The primary antibodies were against the HaloTag protein (Promega, G9281; 1:150), FLAG (Cell Signaling Technology, 2983, 1:400; or Sigma-Aldrich, F1804, 1:250), the LE/Ly marker LBPA (1:20; prepared as described [34]), and LAMP2A (Abcam, ab125068; 1:500). Subsequently, the cells were washed three times with 0.1% BSA in PBS and incubated with an Alexa Fluor 488-conjugated anti-mouse antibody (Abcam, ab150113; 1:1,000) and an Alexa Fluor 647-conjugated anti-rabbit antibody (Abcam, ab150083; 1:1,000). Images were acquired with either a BZ-X710 fluorescence microscope (Keyence, Osaka, Japan) with a 20x objective lens (Fig. S2B) or a TCS SP8 inverted confocal microscope (Leica, Germany) equipped with a 63x oil immersion lens (Figs. S2I-M).

### Protein expression and purification

The N- and C-domains of mouse LAMP1 and LAMP2A were expressed as secreted proteins, by the transient transfection of HEK293 cells lacking N-acetylglucosaminyltransferase I (Gn-TI), and purified as described previously [4]. The isolated N- and C-domains were loaded onto a Superdex 75 10/300 GL column (GE Healthcare, 17-5174-01), equilibrated with 20 mM HEPES-NaOH (pH 7.5) and 150 mM NaCl, and separated at a flow rate of 0.4 ml/min using an AKTAexplorer (GE Healthcare UK Ltd.). The protein concentration of each fraction (0.3 ml) was measured by the BCA

Protein Assay Reagent (ThermoFisher Scientific, 23228), using bovine serum albumin as the standard.

### Site-specific crosslinking and/or incorporation of Aloc-Lys

HEK293c18 cells were cultured on 10 cm dishes ( $6.5 \times 10^6$  cells/dish), one day before transfection. Each amber mutant LAMP1 or LAMP2A gene (3.75  $\mu$ g DNA) was cotransfected into HEK293c18 cells with pcBpaRS ver.1 (3.75  $\mu$ g DNA) [19], together with the wild-type LAMP1 or LAMP2A gene (2.5  $\mu$ g DNA), using the Avalanche-Everyday Transfection Reagent (10  $\mu$ l). For the incorporation of Aloc-Lys, the amber mutant LAMP2A-3xMYC or LAMP2A-3xFLAG gene (2.5 or 2  $\mu$ g DNA, respectively) was cotransfected into HEK293c18 cells with pcPylRS<sup>Y384F,Y306A</sup> (2  $\mu$ g DNA) and pOriPpU6tRNA<sup>Pyl</sup> (3  $\mu$ g DNA) [48]. Four hours after transfection, pBpa or Aloc-Lys was supplemented into the culture medium at a final concentration of 0.46 mM or 3.3 mM, respectively, and the cells were cultured for another 15 h. The cells were then washed with PBS, exposed to UV light for 15 min, and lysed with 1% Triton X-100 in buffer A. Although long irradiation durations over several hours reportedly increase the efficiency of photo-crosslinking [36], in this study the irradiation was shorter, to avoid impairment of the cell viability. Thus, the amounts of the crosslinked products may be less than those of the coimmunoprecipitated monomers. Cell lysates were incubated for 1 hour at 4°C with anti-FLAG M2 agarose resin (Sigma-Aldrich, A2220). After the resin was washed, 60  $\mu$ l of SDS-sample buffer A was added to the resin and the mixture was heated at 100°C for 10 min. For the reductive alkylation, 48  $\mu$ l of SDS-sample buffer, consisting of 750 mM Tris-HCl, pH 8.8, 20 mM dithiothreitol, 2.5% SDS, and 7.5% glycerol (w:v), was added to the washed resin. The resin was heated at 95°C for 10 min, left to cool to room temperature, and then incubated for 30 min in the presence of 40 mM iodoacetamide. After brief centrifugation, the materials eluted from the resin were analyzed by immunoblotting.

### Immunoblotting

The proteins in the lysates and the immunoprecipitated materials (15  $\mu$ l per lane) were fractionated by 5–20% SDS-PAGE (SuperSep<sup>TM</sup> Ace 5–20%; Wako, 197-15011) or 9% SDS-PAGE, and were blotted onto polyvinylidene difluoride membranes in transfer buffer (25 mM Tris, 192 mM glycine, 20% methanol, 0.1% SDS). The blots were probed with the rabbit anti-DYKDDDDK Tag monoclonal antibody (mAb; Cell Signaling Technology, 2368), the rabbit anti-MYC Tag (71D10) mAb (Cell Signaling Technology, 2278) or the mouse anti-HaloTag protein mAb (Promega, G9211), using a horseradish peroxidase (HRP)-conjugated secondary antibody (Abcam, ab205718 or ab205719). Immunoreactivity was detected based on chemiluminescence, using the ECL Blotting Reagents (GE Healthcare Life Sciences, RPN2109) or the ECL prime western blotting system (GE Healthcare Life Sciences, RPN2232), and Hyperfilm ECL (GE Healthcare Life Sciences, 28906836). Densitometric analyses of the band intensities were performed with the Fiji software. The intensity values

obtained within a linear range, where the densitometric profile did not plateau, were used for the quantitative analysis.

In order to compare the crosslinking efficiency among the variant LAMPs with *pBpa* at different positions, the amount of the crosslinked product was normalized by that of the corresponding immunoprecipitated monomer. Since the amounts of the crosslinked products were much less than those of the monomers, the band intensities were separately measured after long and short exposures, respectively. The band intensity of each crosslinked product was then divided by that of the monomer. The numerical values thus obtained are expressed as the ratios to those with mouse LAMP2A<sup>P261X</sup> and LAMP1<sup>P251X</sup> (*X*: *pBpa*).

### PNGase treatment

Mouse LAMP2A-3xFLAG<sup>P261X</sup> or LAMP2A-3xFLAG<sup>R278X</sup> (*X*: *pBpa*) and the wild-type LAMP2A-3xMYC were coexpressed in HEK293c18 cells and subjected to the site-specific photocrosslinking as described above. After immunoprecipitation with anti-FLAG M2 agarose resin, 60  $\mu$ l of denaturing buffer, consisting of 10 mM Tris-HCl, pH 6.8, 8 mM dithiothreitol, and 0.1% SDS, was added to the washed resin. The resin was heated at 100°C for 5 min. After brief centrifugation, a 20  $\mu$ l portion of the materials eluted from the resin was mixed with 30  $\mu$ l of reaction buffer, consisting of 80 mM sodium phosphate, pH 7.5, and 1.6% NP-40 with or without 8,000 U/ml PNGaseF (New England BioLabs, P0704), and incubated 37°C for 1 h. After adding 5  $\mu$ l of 50% glycerol containing 0.05% bromophenol blue (w:v), the materials were fractionated and analyzed by immunoblotting.

### Free-flow electrophoresis

HEK293c18 cells were cultured on 10-cm dishes (6.5  $\times$  10<sup>6</sup> cells/dish), one day before transfection. The cells in ten dishes were transfected with the amber mutant of the mouse *Lamp2-Myc* gene (3.75  $\mu$ g DNA/dish) and *pcpBpaRS* ver.1 (3.75  $\mu$ g DNA/dish). Four hours after transfection, *pBpa* was supplemented into the culture medium at a final concentration of 0.4 mM, and the cells were cultured for another 14 h. The cells were then washed with PBS, exposed to UV light for 15 min, and collected using cell scrapers. The cells were suspended in buffer B, consisting of 10 mM triethanolamine, 10 mM acetic acid, 1 mM EDTA, and 250 mM sucrose, pH 7.4, and disrupted by nitrogen cavitation using a Cell Disruption Vessel (Parr Instrument Company, 4639, Parr Instrument, Moline, IL, USA). The homogenate was centrifuged at 7,700 g for 10 min, and the resulting supernatant was separated by free-flow electrophoresis (FFE) on an OCTOPUS instrument (FFE Service GmbH, Feldkirchen, Germany) [38]. Buffer B was used in the separation chamber, and the unit was operated at 330 ml/h with a field of 600 V. Samples were continuously separated into 24 channels. After the FFE, the organelles in each fraction were recovered by centrifugation at 200,000 g (55,000 rpm) for 40 min at 4°C in an S58A-2057 rotor (himac CS-100FNX, HITACHI, Japan), and analyzed by immunoblotting using the rabbit anti-MYC Tag (71D10) mAb (Cell Signaling Technology, 2278), the mouse anti-

KDEL mAb (Santa Cruz Biotechnology, sc-58774), the rabbit anti-GOLGA5 polyclonal antibody (pAb; SIGMA Life Science, HPA000992), the rabbit anti-LAMP1 antibody (Abcam, ab24170), the mouse anti-CTSD/cathepsin D mAb (Abcam, ab6313), the rabbit anti-AIFM/AIF pAb (Abcam, ab1998) and the rabbit anti-EEA mAb (Cell Signaling Technology, 3288). The immunoblot signals were detected by the FUSION chemiluminescence imaging system (VILBER, Collegien, France).

### Statistical analysis

Differences in the numbers of GAPDH-HT per cell in the four groups were analyzed using the statistical software “EZR (Easy R)” [49]. The numbers were compared by Kruskal-Wallis nonparametric analysis. The Steel-Dwass test was used for post hoc comparisons.

### Acknowledgments

We thank Dr. Gerhard Weber at FFE Service GmbH (Feldkirchen, Germany) and Prof. Noboru Mizushima at The University of Tokyo for assistance with the free-flow electrophoresis experiments. This study was supported by a Nanken-Kyoten grant from TMDU, and a Grant-in-Aid for Scientific Research, 17K12005 (to M.H.).

### Disclosure statement

No potential conflict of interest was reported by the author(s).

### References

- [1] Saftig P, Schroder B, Blanz J. Lysosomal membrane proteins: life between acid and neutral conditions. *Biochem Soc Trans.* 2010;38:1420–1423.
- [2] Chen JW, Cha Y, Yuksel KU, et al. Isolation and sequencing of a cDNA clone encoding lysosomal membrane glycoprotein mouse LAMP-1. Sequence similarity to proteins bearing onco-differentiation antigens. *J Biol Chem.* 1988;263:8754–8758.
- [3] Fukuda M, Viitala J, Matteson J, et al. Cloning of cDNAs encoding human lysosomal membrane glycoproteins, h-lamp-1 and h-lamp-2. Comparison of their deduced amino acid sequences. *J Biol Chem.* 1988;263:18920–18928.
- [4] Terasawa K, Tomabechi Y, Ikeda M, et al. Lysosome-associated membrane proteins-1 and -2 (LAMP-1 and LAMP-2) assemble via distinct modes. *Biochem Biophys Res Commun.* 2016;479:489–495.
- [5] Wilke S, Krausz J, Bussow K. Crystal structure of the conserved domain of the DC lysosomal associated membrane protein: implications for the lysosomal glycoalyx. *BMC Biol.* 2012;10:62.
- [6] Eskelinen EL, Schmidt CK, Neu S, et al. Disturbed cholesterol traffic but normal proteolytic function in LAMP-1/LAMP-2 double-deficient fibroblasts. *Mol Biol Cell.* 2004;15:3132–3145.
- [7] Andrejewski N, Punnonen EL, Guhde G, et al. Normal lysosomal morphology and function in LAMP-1-deficient mice. *J Biol Chem.* 1999;274:12692–12701.
- [8] Tanaka Y, Guhde G, Suter A, et al. Accumulation of autophagic vacuoles and cardiomyopathy in LAMP-2-deficient mice. *Nature.* 2000;406:902–906.
- [9] Eskelinen EL, Cuervo AM, Taylor MR, et al. Unifying nomenclature for the isoforms of the lysosomal membrane protein LAMP-2. *Traffic.* 2005;6:1058–1061.
- [10] Kaushik S, Cuervo AM. The coming of age of chaperone-mediated autophagy, nature reviews. *Mol Cell Biol.* 2018;19:365–381.

- [11] Nishino I, Fu J, Tanji K, et al. Primary LAMP-2 deficiency causes X-linked vacuolar cardiomyopathy and myopathy (Danon disease). *Nature*. 2000;406:906–910.
- [12] Chi C, Leonard A, Knight WE, et al. LAMP-2B regulates human cardiomyocyte function by mediating autophagosome-lysosome fusion. *Proc Natl Acad Sci U S A*. 2019;116:556–565.
- [13] Fujiwara Y, Furuta A, Kikuchi H, et al. Discovery of a novel type of autophagy targeting RNA. *Autophagy*. 2013;9:403–409.
- [14] Fujiwara Y, Kikuchi H, Aizawa S, et al. Direct uptake and degradation of DNA by lysosomes. *Autophagy*. 2013;9:1167–1171.
- [15] Bandyopadhyay U, Kaushik S, Varticovski L, et al. The chaperone-mediated autophagy receptor organizes in dynamic protein complexes at the lysosomal membrane. *Mol Cell Biol*. 2008;28:5747–5763.
- [16] Carvalho P, Stanley AM, Rapoport TA. Retrotranslocation of a misfolded luminal ER protein by the ubiquitin-ligase Hrd1p. *Cell*. 2010;143:579–591.
- [17] Ieva R, Tian P, Peterson JH, et al. Sequential and spatially restricted interactions of assembly factors with an autotransporter beta domain. *Proc Natl Acad Sci U S A*. 2011;108:E383–391.
- [18] Shimizu H, Miyazaki H, Ohsawa N, et al. Structure-based site-directed photo-crosslinking analyses of multimeric cell-adhesive interactions of voltage-gated sodium channel beta subunits. *Sci Rep*. 2016;6:26618.
- [19] Hino N, Okazaki Y, Kobayashi T, et al. Protein photo-crosslinking in mammalian cells by site-specific incorporation of a photoreactive amino acid. *Nat Methods*. 2005;2:201–206.
- [20] Hino N, Hayashi A, Sakamoto K, et al. Site-specific incorporation of non-natural amino acids into proteins in mammalian cells with an expanded genetic code. *Nat Protoc*. 2006;1:2957–2962.
- [21] Chin JW, Cropp TA, Anderson JC, et al. An expanded eukaryotic genetic code. *Science*. 2003;301:964–967.
- [22] Hara-Yokoyama M, Kukimoto-Niino M, Terasawa K, et al. Tetrameric interaction of the ectoenzyme CD38 on the cell surface enables its catalytic and raft-association activities. *Struct (London, England)*. 1993;20(2012):1585–1595.
- [23] Majeski AE, Dice JF. Mechanisms of chaperone-mediated autophagy. *Int J Biochem Cell Biol*. 2004;36:2435–2444.
- [24] Cuervo AM, Dice JF. A receptor for the selective uptake and degradation of proteins by lysosomes. *Science*. 1996;273:501–503.
- [25] Seki T, Yoshino KI, Tanaka S, et al. Establishment of a novel fluorescence-based method to evaluate chaperone-mediated autophagy in a single neuron. *PLoS One*. 2012;7:e31232.
- [26] Sato M, Seki T, Konno A, et al. Fluorescent-based evaluation of chaperone-mediated autophagy and microautophagy activities in cultured cells. *Genes Cells*. 2016;21:861–873.
- [27] Sahu R, Kaushik S, Clement CC, et al. Microautophagy of cytosolic proteins by late endosomes. *Dev Cell*. 2011;20:131–139.
- [28] Hara T, Takamura A, Kishi C, et al. FIP200, a ULK-interacting protein, is required for autophagosome formation in mammalian cells. *J Cell Biol*. 2008;181:497–510.
- [29] Cuervo AM. Chaperone-mediated autophagy: selectivity pays off. *Trends Endocrinol Metab*. 2010;21:142–150.
- [30] Jenkins JL, Tanner JJ. High-resolution structure of human D-glyceraldehyde-3-phosphate dehydrogenase. *Acta Crystallogr, Sect D*. 2006;62:290–301.
- [31] Orlowski M, Cardozo C, Michaud C. Evidence for the presence of five distinct proteolytic components in the pituitary multicatalytic proteinase complex. Properties of two components cleaving bonds on the carboxyl side of branched chain and small neutral amino acids. *Biochemistry*. 1993;32:1563–1572.
- [32] Bai JP. The involvement of cytosolic chymotrypsin-like, trypsin-like, and cucumisin-like activities in degradation of insulin and insulin-like growth factor I by epithelial tissues. *J Pharm Pharmacol*. 1995;47:674–677.
- [33] Los GV, Encell LP, McDougall MG, et al. HaloTag: a novel protein labeling technology for cell imaging and protein analysis. *ACS Chem Biol*. 2008;3:373–382.
- [34] Kobayashi T, Stang E, Fang KS, et al. A lipid associated with the antiphospholipid syndrome regulates endosome structure and function. *Nature*. 1998;392:193–197.
- [35] Matsuo H, Chevallier J, Mayran N, et al. Role of LBPA and Alix in multivesicular liposome formation and endosome organization. *Science*. 2004;303:531–534.
- [36] Sato S, Mimasu S, Sato A, et al. Crystallographic study of a site-specifically cross-linked protein complex with a genetically incorporated photoreactive amino acid. *Biochemistry*. 2011;50:250–257.
- [37] Mukai T, Kobayashi T, Hino N, et al. Adding l-lysine derivatives to the genetic code of mammalian cells with engineered pyrrolysyl-tRNA synthetases. *Biochem Biophys Res Commun*. 2008;371:818–822.
- [38] Katsumata O, Kimura T, Nagatsuka Y, et al. Charge-based separation of detergent-resistant membranes of mouse splenic B cells. *Biochem Biophys Res Commun*. 2004;319:826–831.
- [39] Krivankova L, Bocek P. Continuous free-flow electrophoresis. *Electrophoresis*. 1998;19:1064–1074.
- [40] Bandyopadhyay U, Sridhar S, Kaushik S, et al. Identification of regulators of chaperone-mediated autophagy. *Mol Cell*. 2010;39:535–547.
- [41] Arias E, Koga H, Diaz A, et al. Lysosomal mTORC2/PHLPP1/Akt regulate chaperone-mediated autophagy. *Mol Cell*. 2015;59:270–284.
- [42] Rout AK, Strub MP, Piszczek G, et al. Structure of transmembrane domain of lysosome-associated membrane protein type 2a (LAMP-2A) reveals key features for substrate specificity in chaperone-mediated autophagy. *J Biol Chem*. 2014;289:35111–35123.
- [43] Kato Y, Arakawa S, Terasawa K, et al. The ceramide analogue N-(1-hydroxy-3-morpholino-1-phenylpropan-2-yl)decanamide induces large lipid droplet accumulation and highlights the effect of LAMP-2 deficiency on lipid droplet degradation. *Bioorg Med Chem Lett*. 2020;30:126891.
- [44] Hirst J, Itzhak DN, Antrobus R, et al. Role of the AP-5 adaptor protein complex in late endosome-to-Golgi retrieval. *PLoS Biol*. 2018;16:e2004411.
- [45] Shirane M, Wada M, Morita K, et al. Protrudin and PDZD8 contribute to neuronal integrity by promoting lipid extraction required for endosome maturation. *Nat Commun*. 2020;11:4576.
- [46] Hurley JH, Young LN. Mechanisms of autophagy initiation. *Annu Rev Biochem*. 2017;86:225–244.
- [47] Gan B, Peng X, Nagy T, et al. Role of FIP200 in cardiac and liver development and its regulation of TNFalpha and TSC-mTOR signaling pathways. *J Cell Biol*. 2006;175:121–133.
- [48] Hino N, Sakamoto K, Yokoyama S. Site-specific incorporation of unnatural amino acids into proteins in mammalian cells. *Methods Mol Biol*. 2012;794:215–228.
- [49] Kanda Y. Investigation of the freely available easy-to-use software 'EZR' for medical statistics. *Bone Marrow Transplant*. 2013;48:452–458.
- [50] De Saint-vis B, Vincent J, Vandenebeele S, et al. A novel lysosome-associated membrane glycoprotein, DC-LAMP, induced upon DC maturation, is transiently expressed in MHC class II compartment. *Immunity*. 1998;9:325–336.
- [51] Holness CL, Da Silva RP, Fawcett J, et al. Macrosialin, a mouse macrophage-restricted glycoprotein, is a member of the lamp/lgp family. *J Biol Chem*. 1993;268:9661–9666.
- [52] David A, Tiveron MC, Defays A, et al. BAD-LAMP defines a subset of early endocytic organelles in subpopulations of cortical projection neurons. *J Cell Sci*. 2007;120:353–365.